

# Casein kinase 2 mediated phosphorylation of Spt6 modulates histone dynamics and regulates spurious transcription

Emmanuelle Gouot<sup>1</sup>, Wajid Bhat<sup>1</sup>, Anne Rufiange<sup>1</sup>, Eric Fournier<sup>1,2</sup>, Eric Paquet<sup>1,2,3</sup> and Amine Nourani<sup>1,\*</sup>

<sup>1</sup>Laval University Cancer Research Center, St-Patrick Research Group in Basic Oncology, Québec, Québec, Canada, <sup>2</sup>CHU de Québec Research Center – Laval University, Endocrinology and Nephrology CHUL, Québec, Québec, Canada and <sup>3</sup>The Institute of Bioengineering, School of Life Sciences, École Polytechnique Fédérale de Lausanne, Lausanne, Switzerland

Received April 06, 2018; Revised May 18, 2018; Editorial Decision May 22, 2018; Accepted May 24, 2018

## ABSTRACT

**CK2 is an essential protein kinase implicated in various cellular processes. In this study, we address a potential role of this kinase in chromatin modulations associated with transcription. We found that CK2 depletion from yeast cells leads to replication-independent increase of histone H3K56 acetylation and global activation of H3 turnover in coding regions. This suggests a positive role of CK2 in maintenance/recycling of the histone H3/H4 tetramers during transcription. Interestingly, strand-specific RNA-seq analyses show that CK2 inhibits global cryptic promoters driving both sense and antisense transcription. This further indicates a role of CK2 in the modulation of chromatin during transcription. Next, we showed that CK2 interacts with the major histone chaperone Spt6, and phosphorylates it *in vivo* and *in vitro*. CK2 phosphorylation of Spt6 is required for its cellular levels, for the suppression of histone H3 turnover and for the inhibition of spurious transcription. Finally, we showed that CK2 and Spt6 phosphorylation sites are important to various transcriptional responses suggesting that cryptic intragenic and antisense transcript production are associated with a defective adaptation to environmental cues. Altogether, our data indicate that CK2 mediated phosphorylation of Spt6 regulates chromatin dynamics associated with transcription, and prevents aberrant transcription.**

## INTRODUCTION

All DNA-related processes within the cell such as replication, transcription and repair occur in the context of chromatin. The basic unit of chromatin, the nucleosome, consists of 147 base pairs of DNA wrapped around a histone octamer (1). To make DNA accessible to the various macromolecules involved in the processes listed above, cells need to modulate chromatin structure. Different factors can alter chromatin structure; these include histone modifiers, ATP-dependent chromatin remodelers, histone chaperones and histone variants. Modulation of chromatin structure during transcription elongation has been the focus of several studies [reviewed in (2,3)]. Diverse sets of factors have been identified to play important roles in altering chromatin structure during transcription elongation, e.g. Isw1, Isw2, SWI/SNF, Chd1, Spt6, the FACT complex (Spt16-Pob3), Set2, Set1 and the Paf1 complex [reviewed in (3–5)].

Nucleosomes are a major obstacle to transcription elongation (6). Cells have developed intricate mechanisms involving histone chaperones (HCs) to deal with this challenge. HCs promote disassembly of nucleosomes in front of RNAP II and reassembly in its wake [reviewed in (7–9)]. Chromatin reassembly in the wake of transcription is related to the important issue of dealing with the consequences of RNAP II passage (10,11). The cell must re-establish chromatin structure to repress a large number of sites that should not allow transcription initiation (12–14). The consequences of this spurious transcription are not known. However, it may interfere with many important processes, such as gene regulation, self-renewal of stem cells, genome stability and viral infections (15–18). HCs play an important role in the regulation of spurious transcription

\*To whom correspondence should be addressed. Tel: +418 525 4444 (Ext. 15593) (office), (Ext. 16898) (lab); Fax: +418 691 5439; Email: Amine.Nourani@crchudequebec.ulaval.ca

presumably by reassembling nucleosomes in the wake of RNAP II. Interestingly, recent studies showed that HCs involved in yeast spurious transcription regulation, such as Spt2 and Spt6, use the histone H3/H4 molecules displaced by transcription and recycle them to reassemble nucleosomes following RNAP II passage (19,20). This function is of great importance because it blocks the incorporation of newly synthesized histones that are highly acetylated (21,22) which may contribute to the maintenance of histone marks in transcribed regions. Acetylated histones tend to favor initiation from cryptic promoters located within coding regions. Furthermore, in addition to blocking spurious transcription, nucleosome reassembly mediated by HCs, such as Spt6, prevents wrongful localization of the variant histone H2A.Z in transcribed units (23).

Spt6 is a major conserved H3/H4 HC, essential for the repression of spurious transcription and the maintenance of nucleosomes (12,13,23–27). Many questions regarding the function and regulation of Spt6 remain without answers. Interestingly, we have found that Spt6 interacts with the HC Spt2 and that this interaction is regulated by Casein Kinase 2 (CK2) through the phosphorylation of Spt2 (28). CK2 is an essential serine/threonine kinase involved in many cellular processes [reviewed in (29,30)]. CK2 is commonly deregulated in cancer, and several studies suggest a link between CK2 dysfunction and epigenetic modulations in favor of the tumorigenesis process (31,32). Moreover, it has been shown in different organisms that CK2 interacts with many factors involved in chromatin modulations and may regulate their functions. Studies in *Saccharomyces cerevisiae* (33–35), *Plasmodium falciparum* (36), *Drosophila* (37), and mammals (38) strongly suggest a conserved and extensive role of CK2 in chromatin modulations. However, this role and the concerned molecular mechanisms remain elusive. Importantly, as mentioned previously, we have found that CK2 interacts with Spt2, phosphorylates it and thereby disrupts its interaction with Spt6 (28). We found that this regulation plays a role in the association of Spt2 with coding regions and into the function of this HC in the repression of spurious transcription in yeast. In addition to the link between CK2, Spt2 and Spt6, this kinase has been directly involved in interactions with other factors that are implicated in chromatin modulations during transcription elongation. Indeed, CK2 cooperates with the FACT complex to phosphorylate the PAF complex and may regulate indirectly the level of H2B ubiquitylation in coding regions (33,39). Proteomic analyses show that it also co-purifies with Spt4/Spt5, FACT and other elongation related factors (35,40). Together, these observations strongly suggest a potential role of CK2 in chromatin dynamics during transcription elongation.

In this study, we have specifically addressed the role of CK2 in chromatin dynamics associated with transcription. Using ChIP and ChIP-seq approaches, we have found that CK2 regulates histone H3 dynamics outside of replication, indicating a role in nucleosomes turnover associated with transcription. In cells depleted of CK2 activity, newly synthesized histone H3 are incorporated in transcribed regions at a higher rate than what should be expected in normal cells. As a consequence, cryptic sense and antisense transcripts levels are increased in these cells, indicating that chromatin refolding in transcribed units is deficient. We

next addressed the question of how CK2 regulates this process. We reasoned that CK2 could regulate the function of key factors that are involved in chromatin dynamics associated with transcription. Importantly, we found that it interacts and phosphorylates the HC Spt6, which plays a major role in chromatin refolding during transcription elongation (12,13,20,23,26). Furthermore, we identified the CK2 phosphorylation sites in Spt6 and showed that mutation of these sites affects the function of this protein. Interestingly, our global analyses of transcripts by RNA-seq indicate that CK2 phosphorylation sites are involved in the regulation of cryptic sense and antisense transcription. Moreover, comparison between CK2 and Spt6 mutant data sets clearly shows that both regulate the levels of similar cryptic transcripts suggesting an overlapping function. Surprisingly, we found that Spt6 cellular levels are directly controlled by CK2 and their restoration bypass the need for normal CK2 activity for the repression of cryptic transcription. Finally, we show that CK2 and Spt6 phosphorylation are required for the dynamic response to environmental changes and various stresses. Taken together, our data show that CK2 regulates the dynamics of chromatin in transcribed regions by modulating Spt6 stability.

## MATERIALS AND METHODS

### *Saccharomyces cerevisiae* strains and plasmids

All strains used in this study are isogenic to S288C (41) and are listed in Supplementary Table S1. Strains were constructed by standard genetic methods, either by crosses or by transformation. Yeast cells expressing different *SPT6* alleles were constructed by transformation of *SPT6* plasmid containing the indicated alleles in *SPT6/Δspt6* diploid strains followed by tetrad dissection. *SPT6-FLAG*, *CKA1-13MYC*, *CKA2-13MYC*, *IWS1-13MYC*, *CKB2-TAP*, alleles were constructed by integrating the DNA encoding the particular epitope at the 3'-end of the respective gene (42,43). The *cka1Δ::KANMX6*, *spt6Δ::KANMX6* and *bar1Δ::NatMX4* alleles were constructed by replacing the open reading frame with *KANMX6* or *NatMX4* selection marker (42,44). The point mutation in the *CKA2* allele (D225N) was introduced as described in (45) with *NatMX6* as a selection marker. The plasmids were constructed using standard molecular biology techniques. 6-His fusion plasmids were constructed by insertion of PCR amplified fragments into the appropriate sites of the pet15b vectors (Novagen). The pCC11 *SPT6* WT plasmid is described elsewhere (46). Plasmids expressing Spt6 were generated by mutagenesis of pCC11 using Quick Change Multi Site-Directed Mutagenesis Kit from Agilent Technologies following the manufacturer's protocol. All mutations were verified by sequencing. *FLAG-SPT6* was amplified from genomic DNA and inserted in the YCp50 plasmid. Plasmid YCp has been described elsewhere (47). Growth of different strains was monitored by spot tests on the indicated medium

### Western blot and antibodies

Proteins were extracted in the presence of trichloroacetic acid, separated on 8–15% SDS-PAGE gels, and transferred

to nitrocellulose membrane. Membranes were incubated with anti p-Ser5 (Millipore clone 3E8, 04-1572), anti p-Ser2 (Millipore clone 3E10, 04-1571), anti Rpb1 (8WG16 Covance, MMS-126R), anti Pkg1 (Invitrogen 459250) anti-H3 (Abcam Ab1791), anti-H3K36me3 (Abcam Ab9050), anti-Flag (Sigma F3165), anti-Myc (Covance MMS-150R), anti-Tap (Open Biosystems CAB1001) and anti His (Clontech 631212). Ponceau red staining and Pkg1 signal were used to determine equal loading.

### Protein purification and *in vitro* phosphorylation assay

Recombinant 6His-tagged proteins were expressed in *Escherichia coli* BL21 bacteria and purified with Ni<sup>2+</sup>-nitrilotriacetic acid (NTA)-agarose (Qiagen) according to the manufacturer's protocol. Tandem affinity purification (TAP) of Ckb2 was done as described previously (43). *In vitro* phosphorylation of recombinant proteins was done as described previously (28). His-tagged recombinant proteins (1 µg) were incubated for 30 min at 30°C with CK2 purified from yeast in kinase buffer (final concentration of 80 mM NaCl–KCl, 25 mM Tris–HCl [pH 8], 10 mM MgCl<sub>2</sub>, 1 mM DTT, 50 µM cold ATP and 1 µCi [ $\gamma$ -<sup>32</sup>P]ATP). Samples were run on 10% SDS-PAGE gels, blotted onto nitrocellulose, dried and exposed to film.

### Immunoprecipitation experiments

Co-immunoprecipitation assays were performed as described previously (48). Briefly, 10 µl of anti-Flag M2 agarose beads were incubated overnight at 4°C with yeast whole-cell extract (WCE) (5 mg of total protein) in binding buffer (20 mM HEPES [pH 7.5], 300 mM NaCl, 10% glycerol, 0.1% NP-40, 2 µg/ml of leupeptin and pepstatin, 5 µg/ml of aprotinin and 1 mM phenylmethylsulfonyl fluoride [PMSF]). Beads were washed three times with the binding buffer. Bound proteins were analyzed by Western blotting. For His pulldown assay, 300 ng of recombinant 6xHis-Spt6 coupled to Ni-NTA agar beads were incubated with an equal amount of Ckb2-TAP purified from yeast in pull-down buffer (20 mM Hepes (pH 7.5), 150 mM NaCl, 10% glycerol, 100 µg/ml BSA, 0.5 mM DTT, 0.1% NP-40 and 2 µg/ml each of leupeptin and pepstatin, 5 µg/ml aprotinin) for 3 h at 4°C. Beads were washed three times with pull-down buffer and bound proteins were analyzed by western blot with an antibody against TAP-tag.

### Protein stability assay

Cells were grown to mid-log phase in synthetic medium with 2% glucose as the carbon source and reinoculated in 50 ml fresh media with 0.003% SDS at OD<sub>600</sub> 0.5 for 3 h. Then, cultures were shifted to 37°C, cycloheximide (Sigma, 7698) was added to a final concentration of 40 µg/ml to stop protein synthesis and cells were harvested at different time points. Cell lysates were prepared in lysis buffer and protein concentration was determined using the Bradford assay. Proteins were analyzed by SDS-PAGE and western blotting using the same amount of total proteins for each time point.

### Transcriptional response assays

For galactose induction, strains were grown in YP 2% raffinose, to an OD<sub>600</sub> of 0.8, G1 arrested with  $\alpha$  factor and shifted to 37°C for 30 min. Then, galactose was added to a final concentration of 2% and cells were harvest at the indicated time. For amino-acid starvation, cells were grown in synthetic media lacking histidine (SC-HIS) to an OD<sub>600</sub> of 0.8 and shifted or not to 37°C for 30 min. Then, 3-aminotriazole (3AT, Sigma A8056) was added to the final concentration of 40 mM and cells were harvest after 1 h of treatment.

### Chromatin immunopurification (ChIP)

ChIP experiments were performed as described previously (21). Efficient G1 arrest (at least 95%) of yeast cells was achieved by adding 500 ng/ml  $\alpha$  factor for 2–3 h. Immunoprecipitation of Rpb1 was performed using 2–3 µg of the 8WG16 anti-CTD antibody per immunoprecipitation (Covance, MMS-126R). Antibodies against p-Ser5 (3E8, 04-1572) and p-Ser2 CTD (3E10, 04-1571) were purchased from Millipore and ChIP was performed using 2 µg per immunoprecipitation. The immunoprecipitations of H3 and H3K56ac were done with 0.5 µg of anti-H3 antibody per immunoprecipitation (Abcam, 1791) and 0.2 µg of anti-H3K56 antibody per immunoprecipitation (Millipore, 07-677-I), respectively. Anti H3K36me3 (Abcam, 9050) were used at 0.5 µg per immunoprecipitations. Finally, the Flag ChIPs were done using 10 µl of anti-Flag agarose beads per immunoprecipitation (Sigma, A2220), and Myc ChIPs were done using 3–5 µg of anti-Myc 9E10 per immunoprecipitation (Covance monoclonal antibodies, MMS-150R). ChIP experiments were analysed by qPCR with oligonucleotides listed in Supplementary Table S2. All ChIP experiments were done at least in triplicates; *P* value < 0.05 (\*), *P* value < 0.01 (\*\*), and *P* value < 0.001 (\*\*\*)

### RNA analyses

Total RNA was isolated using the hot-phenol method. In northern blot analyses, 20 to 40 µg of RNA were separated on a 1% agarose formaldehyde–MOPS gel and transferred to a nylon membrane. The *FLO8*, *SCR1*, *DDC1*, *SPB4*, *PHO84* and *YML122C* probes were amplified by PCR and radiolabeled by random priming. For RT-quantitative PCR (qPCR) quantifications, cDNAs were generated using the Invitrogen M-MLV reverse transcriptase kit and their levels were measured by real-time PCR using LightCycler 480 Sybr green I master kit purchased from Roche. Sequences and detailed protocols used in RT-qPCR are available in online supplementary file. All RT-qPCR experiments were done at least in triplicates; *P* value < 0.05 (\*), *P* value < 0.01 (\*\*), and *P* value < 0.001 (\*\*\*) are indicated. RNA-seq experiments were performed following TruSeq stranded total RNA illumina protocol and Illumina next generation sequencing was performed as 50 base pairs single-end reads (TruSeq was performed at the McGill University and Génome Québec Innovation Centre, Montréal, Canada).

## RNA-seq data processing

The sequenced reads from each sample were preprocessed with Trimmomatic (49) and aligned with bwa (50) to *S. cerevisiae* genome assembly R64-1-1 (GCA\_000146045.2). The number of reads for each exon annotated in Ensembl Release 77 was calculated for both the sense and antisense strands. Differential expression of gene was assessed using DESeq (51). The subset of reads falling within the 5'-most and 3'-most 10% of each exon were also calculated. To avoid confounding effects from non-cryptic antisense transcription, overlapping genes were excluded from further analyses. Furthermore, to reduce the amount of noise from inactive genes, genes with fewer than 20 reads in their 5' region or 10 reads in their 3' region were also excluded (2670 genes in total). For each gene, the following metrics were calculated: antisense ratio =  $\log_2(\text{reads}_{\text{antisense}}/\text{reads}_{\text{sense}})$ , antisense enrichment = antisense ratio<sub>CK2/Spt6</sub> - antisense ratio<sub>WT</sub>, three prime ratio =  $\log_2(\text{reads}_{3'}/\text{reads}_{5'})$  and three prime enrichment = three prime ratio<sub>CK2/Spt6</sub> - three prime ratio<sub>WT</sub>. Additionally, using samtools (52), all libraries were split into sense and antisense reads according to the underlying genes. Coverage of all genes over a hundred equal-sized bins were then calculated using the bam Coverage and compute Matrix utilities from the deeptools suite (53). The average coverage over all genes from the TSS to the TES were then normalized into reads per million (RPM) and plotted for each library.

## ChIP-Seq analyses

Illumina next generation sequencing was performed as 50 base pairs single-end reads at the McGill University and Génome Québec Innovation Centre, Montréal, Canada. The sequenced reads were aligned to the *S. cerevisiae* genome assembly R64-1-1 (GCA\_000146045.2) using bowtie v0.12.8 (54) (Coverage was calculated using bedtools (<http://bedtools.readthedocs.io/>) (55) and was normalized into reads per million (RPM). Metagenes plotting the average coverage for every gene going from transcription start site (TSS) to transcription end site (TES) were then produced using the ngs.plot tool version 2.08 (56). Briefly, we used the ngs.plot.r function with the sarCer3 database, the gene body option and a window of 1000 bp around the gene.

## RESULTS

### CK2 regulates replication-independent H3K56 acetylation in transcribed regions

Several reports involved CK2 functionally and physically with chromatin regulators including Spt2 and Spt6 histone chaperones (28,34,35,38). Importantly, we and others found that Spt2 and Spt6 maintain the histone H3/H4 tetramer in coding regions by repressing replication-independent H3 exchange and turnover at several genes (19,20,57). Whether CK2 is implicated in histone H3 dynamics is not known. In order to address this question, we analyzed, *in vivo*, the role of CK2 in the regulation of H3/H4 exchange in G1 arrested cells. Because histone H3/H4 turnover is tightly associated with H3K56ac levels outside of S-phase (21), we first assessed by ChIP assays the level of H3K56ac in G1 arrested

cells in wild-type or *ck2<sup>ts</sup>* mutant. As shown in Figure 1A, depletion of CK2 activity is associated with higher levels of new H3K56ac in the coding regions of transcribed genes *PMAI*, *CLN3* and *ACT1*. In contrast, no such effect was observed in the non-transcribed intergenic region of chromosome V. Thus, our data suggest that CK2 controls the histone H3 exchange.

### CK2 prevents global histone exchange in 3' end of genes independently of H3K36me3

We tested directly the H3 exchange (Figure 1B and C) by measuring the level of newly synthesized histone Flag-H3 incorporation at various locations in G1 arrested cells as described previously (21). Upon galactose induction in G1 arrested cells, Flag-H3 is synthesized and incorporated in the genome, mainly within the 5' and 3' transcribed regions and not in the coding regions of genes (21,58). ChIP-qPCR assays showed that similarly to H3K56ac, depletion of CK2 resulted in higher incorporation of new Flag-H3 into coding regions of active genes (Figure 1C). This observation confirms that CK2 prevents histone exchange in the coding regions of *PMAI*, *ACT1* and *CLN3* genes. Then, we analyzed the global exchange in wild-type and *ck2<sup>ts</sup>* by Flag-H3 ChIP-seq in G1 arrested cells. Metagenes analyses of replication-independent Flag-H3 incorporation indicated that CK2 inhibition led to increased levels of new H3 association (Figure 1D). This experiment was performed twice with similar results as shown in Supplementary Figure S1A. Interestingly, this effect was globally localized in 3' end of the coding regions of genes as further illustrated in Figure 1E showing two different regions containing *ATP1* and *ACO1* genes. Importantly, previous studies indicated that histone H3 exchange in 3' end of genes is regulated by H3K36 tri-methylation (H3K36me3) mediated by Set2 (22). Our observation suggested the possibility that CK2 could modulate the H3 exchange by regulating directly or indirectly H3K36me3. To address this possibility, we analyzed the effect of CK2 depletion on the global level of H3K36me3 in yeast cells. As indicated in Supplementary Figure S1B, the level of H3K36me3 in restrictive conditions was similar to that of the wild-type. Moreover, H3K36me3 ChIP assays at various genes indicated that CK2 is not involved in the modulation of this histone mark (Supplementary Figure S1C). Thus, our data indicate that CK2 effect on histone H3 dynamics is independent of H3K36me3.

### CK2 inhibition affects global redistribution and phosphorylation of RNAP II

CK2's role in histone H3 dynamics outside of S-phase may suggest a global involvement of this kinase on transcription by RNAP II. Because replication-independent histone H3 exchange is correlated with transcription by RNAP II (21,58), it is possible that the H3 dynamics observed in *ck2<sup>ts</sup>* mutants is the result of a change in RNAP II level, distribution or activity. To address this question, we analyzed the association of RNAP II by Rpb1 ChIP-seq in wild-type and *ck2<sup>ts</sup>* cells in the same conditions described for Flag-H3 experiments. The reads obtained after Rpb1 ChIP-seq were

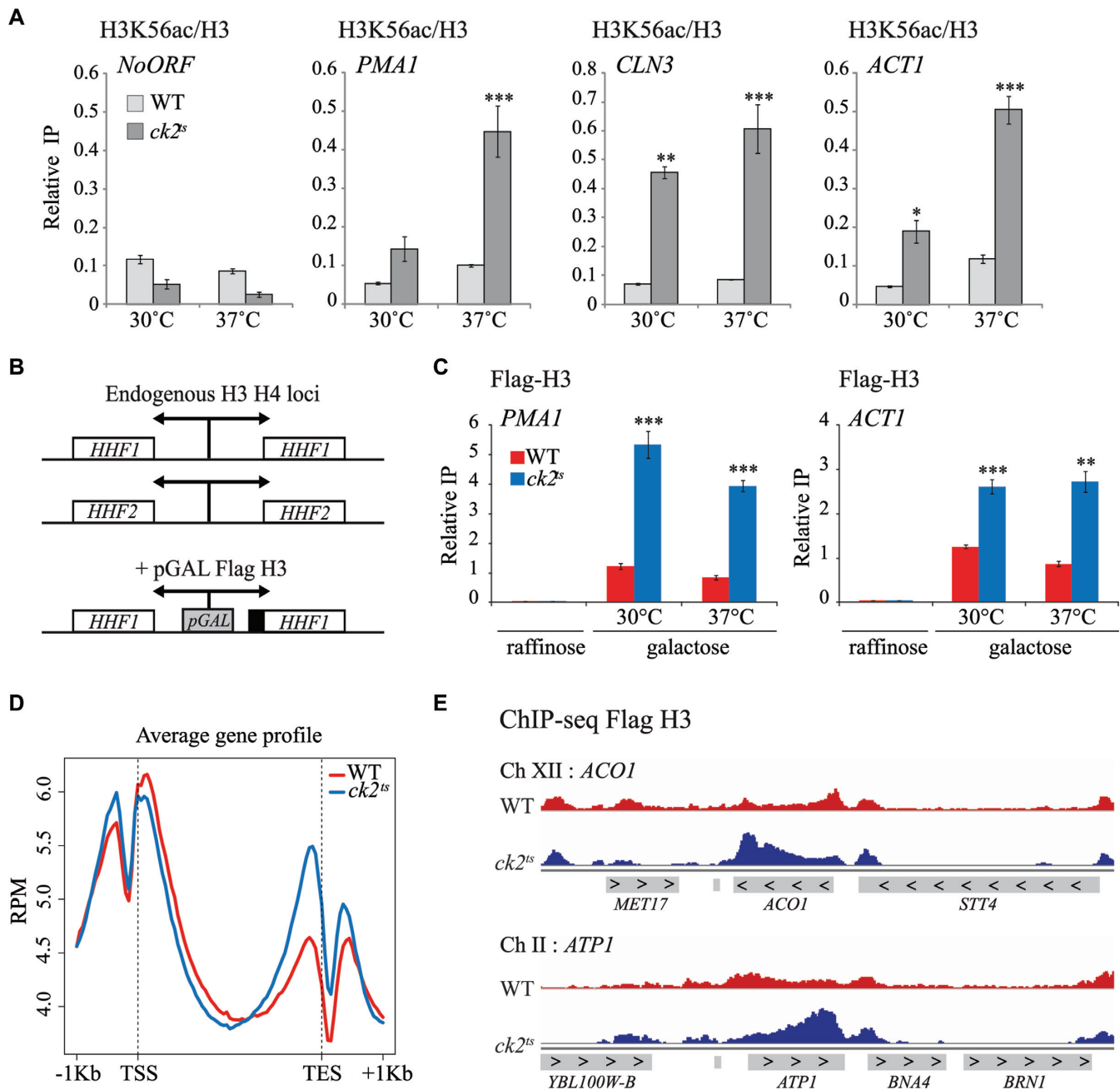


**Figure 1.** Histone H3 turnover is increased in *ck2<sup>ts</sup>* mutant at coding regions of genes. (A) CK2 is required for the repression of replication-independent H3K56ac incorporation. ChIP assays assessing the H3K56 acetylation level in WT and *ck2<sup>ts</sup>*. Cells were G1-arrested and subsequently grown for 2 h at 30 or 37°C. The values shown represent the average and standard errors of three independent experiments measuring H3K56ac levels (IP/Input) relative to histone H3 occupancy (IP/Input). Coding regions of different genes were tested and NoORF is a non-transcribed control locus of chromosome V. (\*) *P* value < 0.05; (\*\*) *P* value < 0.01; (\*\*\*) *P* value < 0.001. (B) Schematic representation of Flag-H3 inducible construction in YAN1104 and YAN1105 strains. A galactose-inducible form of H3, inserted in URA3 locus, was fused to Flag epitope and co-expressed with histone H4. (C) CK2 is required for the replication-independent repression of the new H3 deposition. ChIP experiment of newly synthesized Flag-H3 in WT and *ck2<sup>ts</sup>*. Cells were grown at 30°C in YP-Raffinose, arrested in G1, and then Galactose was added to induce Flag-H3 synthesis for 1 h at 30 or 37°C. The values shown represent the average and standard errors of three independent experiments measuring Flag-H3 (IP/Input) in coding regions of two transcribed genes. (\*) *P* value < 0.05; (\*\*) *P* value < 0.01; (\*\*\*) *P* value < 0.001. (D) CK2 represses global replication-independent incorporation of newly synthesized H3 in the 3' end of genes. Metagenesis of ChIP-seq data showing newly synthesized Flag-H3 signal of WT and *ck2<sup>ts</sup>* strains aligned over transcribed regions of genes. Transcription start site (TSS) and transcription end site (TES) are shown. (E) A view of Flag-H3 ChIP-seq data at two genomic regions of chromosomes XII and II illustrating increased Flag-H3 in *ck2<sup>ts</sup>*.

aligned for each strain on the transcription start site (Supplementary Figure S2A). In contrast to new H3 deposition, we did not observe a consistent change in the global Rpb1 distribution upon CK2 loss. We next grouped the genes with respect to their RNAP II level and analyzed the effect of CK2 on Rpb1 distribution. As shown, in all groups, CK2 depletion had no effect on the pattern of Rpb1 distribution (Supplementary Figure S2B). We also tested the phosphorylation level of cellular Rpb1 in presence or absence of CK2 activity. Interestingly, CK2 depletion led to global decrease in the phosphorylation of CTD-Serine 2 (Supplementary Figure S2C). This suggests that CK2 may affect RNAP II activity.

### CK2 inhibits antisense transcription

The role of CK2 in histone H3 dynamics, RNAP II distribution and phosphorylation suggests a potential global involvement of this kinase in the regulation of transcription. To identify a possible role of CK2 on transcripts levels, we performed strand-specific RNA-seq comparing WT to *ck2<sup>ts</sup>* at restrictive temperature. Strikingly, a CK2-depletion led to an increase of antisense transcripts levels in a large number of genes (Figure 2A). The genes for which the antisense transcript levels were up are overrepresented. The number of genes showing more antisense transcripts is nine times higher than those having antisense transcript levels down. This ration up/down of 9:1 is much higher to what could be expected when we compare it with the gene count of up/down sense ratio that is approximately of 1:1 (*P* value of  $10e^{-70}$ ). Next, we compared wild-type and *ck2<sup>ts</sup>* RNA-seq datasets. Wild-type and *ck2<sup>ts</sup>* sense transcripts showed high level of similarity. However, the Pearson correlation between WT antisense transcripts and *ck2<sup>ts</sup>* was significantly reduced (Figure 2B). This effect to antisense transcripts levels was further confirmed by metagene analysis aligning sense and antisense transcripts to the transcription unit (Figure 2C; Supplementary Figure S3). Antisense enrichment relative to WT has been calculated for each gene in *ck2<sup>ts</sup>* mutant, and 1430 genes showed at least 2-fold increase in their antisense ratio. This experiment was performed twice with similar results each time and the correlation between the two experiments is excellent ( $r = 0.98$ ) as shown in Supplementary Figure S4. To validate the RNA-seq data regarding the altered antisense transcription, we analyzed a locus located in chromosome XIII containing *PHO84* and *YML122C* genes (Figure 2D). *PHO84* antisense transcription produces a long transcript that extend into *YML122C* (15,59). We conducted Northern blot analyses of *PHO84* and *YML122C* in WT and *ck2<sup>ts</sup>* cells. In the conditions of our experiment, *YML122C* is not transcriptionally active and no sense or antisense transcripts from this gene were observed in WT cells. However, depletion of CK2 resulted in the production of a long antisense transcript (*PHO84-YML122C*) starting in *PHO84* and extending into *YML122C* (Figure 2E). The observation of the transcript in *ck2<sup>ts</sup>* cells confirms the RNA-seq data obtained for this locus and further indicates that CK2 inhibits antisense transcription.

### CK2 represses sense spurious transcription from intragenic cryptic promoters

Recent studies highlighted the role of many chromatin remodelers and HCs in the repression of cryptic transcription and established a clear link between chromatin structure regulation in the transcription unit and the repression of both antisense and sense cryptic transcription from within coding regions (13,23,27,60). Because CK2 regulates antisense transcription similar to chromatin regulators, we wanted to know if CK2 depletion was also associated with sense spurious transcription from known cryptic promoters. For that, we first analyzed *FLO8* model gene containing well characterized sense cryptic promoters in its coding region (12,26). *FLO8* cryptic promoters are activated when chromatin is not properly refolded after RNAP II passage (12,26,61). Northern blot analyses were performed on total RNA isolated from wild-type, *ck2<sup>ts</sup>* and *spt6-1004* cells as control (Figure 2F). These analyses showed high levels of *FLO8* short cryptic transcripts in *spt6-1004* cells grown at restrictive temperature, indicating the activation of the sense cryptic promoters. Interestingly, in the *ck2<sup>ts</sup>* cells, we observed strong signals indicating the presence of short cryptic transcripts. Thus, CK2 plays a crucial role in the repression of spurious transcription from *FLO8* cryptic promoters and contributes in the maintenance of proper chromatin structure in its coding region. We next analyzed our RNA-seq data to look for a potential global role of CK2 in the regulation of intragenic spurious transcription. Previous studies showed that derepression of sense cryptic intragenic transcription results in the enrichment of transcripts initiated in the 3' end of genes leading to a global alteration in the 3'/5' transcripts ratio signal (12,27). To address the role of CK2 in cryptic transcription, we generated a ratio of 3' over 5' RNA-seq sense signal to obtain a value for each gene. These values were highly reproducible as shown by the pairwise correlations between each replicate (Supplementary Figure S5). When comparing WT and *ck2<sup>ts</sup>* 3'/5' ratios, we identified 591 genes in *ck2<sup>ts</sup>* with 50% increase (Supplementary Table S3). Representative genes with altered ratio or 3' enrichment relative to WT are shown in Figure 2G. To validate our results, we used different approaches. First, we assessed the 3'/5' expression ratio by RT-qPCR at two other genes exhibiting, in our RNA-seq data, a substantial 3' enrichment in *ck2<sup>ts</sup>*, *SPO23* and *MAL33*. *FLO8* is used as positive 3' enrichment control, *PMAL1* and *FKS1* as negative 3' enrichment controls (Figure 2H). As expected for *FLO8*, *SPO23* and *MAL33*, CK2 depletion led to an alteration in the 3'/5' transcript ratio suggesting that this kinase represses cryptic transcription from within these genes. As a second approach to further confirm our analyses, we tested spurious transcription by Northern blot probing specific genes. Our RNA-seq data predicted spurious initiation at *DDC1* and *SPB4* in *ck2<sup>ts</sup>* mutant. Interestingly, several spurious cryptic transcripts produced from these genes were identified in previous studies (12,27). Using 3' end specific probes, we found clear bands indicating short transcripts initiated from cryptic promoters of *FLO8*, *DDC1* and *SPB4* (Figure 2I). These observations further confirm that CK2 is essential for the repression of spurious tran-

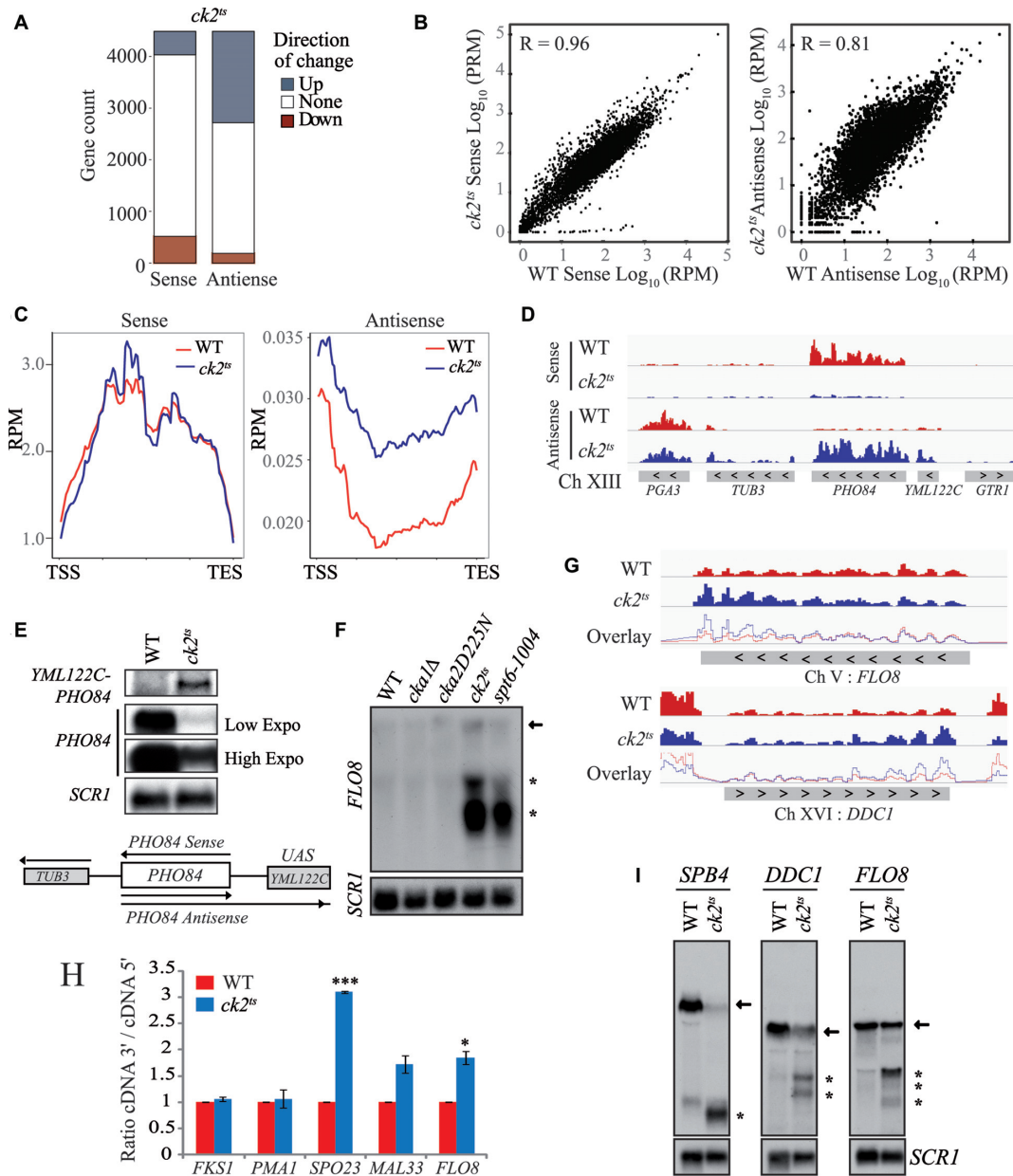


**Figure 2.** CK2 regulates transcriptional accuracy. (A) CK2 is required for the repression of antisense transcription in a high number of genes. A representation of genes count affected by at least two-fold either positively (blue) or negatively (red) in *ck2<sup>ts</sup>* for sense or antisense transcripts levels. (B) The *ck2<sup>ts</sup>* antisense transcripts are less similar to those of wild-type (WT) strain. WT and *ck2<sup>ts</sup>* sense (left panel) or antisense (right panel) log<sub>10</sub> RPM scores were plotted for each transcription unit. The Pearson correlation (*R* value) was calculated and is shown in each panel. (C) CK2 represses global antisense transcription. Metagenome analysis showing WT and *ck2<sup>ts</sup>* RNA-seq RPM signals of the sense (left panel) or antisense (right panel) strands aligned over transcribed regions of genes. Transcription start site (TSS) and transcription end site (TES) are shown. (D) A view of *PHO84* locus (chromosome XIII) sense and antisense strands transcripts data obtained by RNA-seq in WT (red) or *ck2<sup>ts</sup>* (blue). (E) CK2 represses antisense transcription at the *PHO84* locus. Northern blot analyses of *PHO84*-*YML122C* locus transcripts using different probes. *PHO84* probe was used to identify *PHO84* sense transcripts while *YML122C* probe was used specifically to follow the long antisense transcript that starts in *PHO84* and extends into *YML122C*. As shown, this transcript is only observed in *ck2<sup>ts</sup>*. (F) CK2 is required for the suppression of spurious transcription from the cryptic promoter of *FLO8* gene. Total RNA was isolated from WT, *cka1Δ*, *cka2D225N*, *ck2<sup>ts</sup>* and *spb6-1004* cells grown at 30°C and shifted to 37°C for 2 h. The probe for the northern analysis was generated against 3'-end of *FLO8*, and *SCR1* was used as a loading control. The arrow indicates full-length *FLO8* RNA transcripts, and the asterisk indicates *FLO8* short transcripts resulting from cryptic initiation. (G) CK2 mutation leads to 3' enrichment of sense transcripts at *FLO8* and *DDC1*. The sense strands transcripts data were obtained by sequencing total RNA of WT (red) or *ck2<sup>ts</sup>* (blue). The overlay of WT and *ck2<sup>ts</sup>* signals illustrates the 3' RNA enrichment in *ck2<sup>ts</sup>* mutants. (H) CK2 mutation leads to 3' enrichment of sense transcripts at *SPO23*, *MAL33* and *FLO8*. In this experiment, transcripts levels of the indicated genes were analyzed by RT-qPCR. The 5' and 3' regions of each gene were amplified and the values shown are 3'/5' ratios representing the average and standard errors of three independent experiments. (\*) *P* value < 0.05; (\*\*\*) *P* value < 0.001. (I) CK2 is required for the repression of spurious transcription at *DDC1* and *SPB4*. Total RNA was isolated from cells after two hours of growth at 37°C and analysed by Northern Blot with probes specific for 3'-end of *FLO8*, *DDC1* and *SPB4*. *SCR1* was used as a loading control. Arrows indicate full-length RNA transcripts, and asterisks indicate short transcripts.

scription from cryptic promoters located within the coding regions of genes.

### CK2 interacts with and phosphorylates the transcription elongation associated histone chaperone Spt6

Our data indicate a global role of CK2 in the modulation of chromatin structure during transcription elongation. We wanted to address how CK2 regulates this process. Several observations initially suggested that CK2 might fulfill this function at least in part by regulating Spt6 activity. First, Spt6 is one of the most important chromatin organizers in the coding regions of genes throughout evolution (13,16,62). Second, we established that CK2 regulates the Spt6-Spt2 interaction during elongation (28). Third, peptides from the various subunits of CK2 have been identified by mass spectrometry in tandem affinity-purified Spt6 samples (35,40). Fourth, Spt6 was found phosphorylated at three CK2 consensus motifs (35). To investigate the functional relationship between CK2 and Spt6, we first assessed whether this kinase stably interacts with Spt6 *in vivo*. For this purpose, we purified FLAG-Spt6 from yeast strains containing two epitope-tagged CK2 subunits. CK2 subunits Cka1-Myc and Cka2-Myc co-purified with FLAG-Spt6 (Figure 3A). To test if this interaction was direct, we performed a His pulldown assay using purified 6xHis-Spt6. Ckb2 purified from yeast by TAP was incubated with 6xHis-Spt6 coupled with Ni-NTA agarose. As shown in Figure 3B, Ckb2-TAP was pulldown by 6xHis-Spt6 indicating a direct interaction between the histone chaperone and the kinase.

We next determined whether Spt6 was directly phosphorylated by CK2 using an *in vitro* phosphorylation assay with recombinant 6xHis-Spt6 and tandem affinity-purified Ckb2 from yeast. CK2 was able to incorporate  $[\gamma]$ -<sup>32</sup>Pi into Spt6 (Figure 3C). This indicates that Spt6 is a direct substrate for CK2. Interestingly, it has been previously shown that Spt6 is phosphorylated *in vivo* at various CK2 consensus motifs (35,63). To investigate if Spt6 is modified by CK2 *in vivo*, we immunopurified FLAG-Spt6 from WT and *ck2<sup>ts</sup>* yeast strains and analyzed the purified material by Western blot with an antibody against phospho-serine/threonine. As shown in Figure 3D, Spt6 was recognized by the anti-phospho-serine/threonine in WT extracts, further confirming that Spt6 is indeed a phosphoprotein *in vivo*. This signal was significantly altered in the *ck2<sup>ts</sup>* mutant at the restrictive temperature, suggesting an important role for CK2 in the regulation of the phosphorylation state of Spt6 *in vivo*. Taken together, our data indicate that CK2 interacts directly with Spt6 and phosphorylates this elongation factor both *in vitro* and *in vivo*.

Next, we aimed to identify the sites in Spt6 that are phosphorylated by CK2. Previously, three potential CK2 phosphorylation sites (S94, S134 and S206) in Spt6 were shown to be modified *in vivo* (35). We analyzed by mass spectrometry the phosphorylation profile of Spt6 and confirmed that at least two sites (S94, S134) were indeed modified *in vivo* (Supplementary Figure S6). Interestingly, our mass spectrometry analyses allowed the identification of at least one additional site in N-terminal region of Spt6: S155 (Supplementary Figure S6). Moreover, five CK2 phosphorylation

target sites have been reported for Spt6 *in vivo* (63,64). Notably, all the above-mentioned phosphorylation sites are located in the N-terminal region of Spt6. Furthermore, using the NetPhos 3.1 server, we predicted a total of 7 'high score' potential CK2 target sites in the N-terminal region of Spt6 (Figure 3E). We therefore elected to mutate either the three initially identified, or all seven potential CK2 target sites to alanine residues to produce and collect the resulting recombinant protein. Then, we subjected the two mutant proteins to *in vitro* phosphorylation by purified CK2 from yeast. The Spt6 mutant in which the three initial CK2 target sites had been eliminated, exhibited a reduced but residual level of phosphorylation, while no  $[\gamma]$ -<sup>32</sup>Pi was incorporated into a mutant Spt6 protein in which all seven CK2 potential target sites had been eliminated, indicating that these sites include all CK2 phosphorylation sites used *in vitro* (Figure 3F).

### CK2 Phosphorylation in Spt6 are important for its chromatin function

To analyze the potential function of the identified CK2 target sites, we constructed strains expressing Spt6-7SA mutant form and probed a set of phenotypes associated with Spt6 function. One aspect of the *SPT* phenotype is a defect in Spt6 function that suppresses  $\delta$  insertion mutations in the promoter of the *LYS2* genes. Thus, a WT strain with a *lys2-1288* allele is unable to grow in the absence of lysine. A defect in Spt6 function suppresses this phenotype and the strain is no longer auxotrophic for lysine (46). As shown in Figure 4A, cells expressing *spt6-7SA* mutant exhibited thermosensitivity, and an *spt-* phenotype (loss of lysine auxotrophy) on SC-Lys. An *spt-* phenotype indicates defect in Spt6 function associated with chromatin organization (65). Defective Spt6 function is also associated with spurious transcription from cryptic promoters within the coding regions of transcriptionally active genes (12). We analyzed the consequence of the expression of non phosphorylatable Spt6 mutant on the repression of intragenic cryptic promoter at *FLO8* using the reporter system *pGALI-FLO8-HIS3*. The expression from the *FLO8* cryptic promoter, as measured by growth in the absence of histidine, indicates spurious transcription (Figure 4B), reflecting a defect in chromatin refolding during transcription. We also analyzed cryptic transcription at *FLO8* by Northern blot and detected short cryptic transcripts in yeast expressing *spt6-7SA* (Figure 4C). This result shows that CK2 target sites found in the N-terminal region of Spt6 are important for Spt6 chromatin functions. Finally, we assessed by ChIP assays the level of H3K56ac in G1 arrested cells in WT or *spt6-7SA* mutant (Figure 4D). Importantly, the inhibition of Spt6 phosphorylation by CK2 was associated with higher specific incorporation of new H3K56ac in the coding regions of transcribed genes (non-transcribed intergenic region of chromosome V was used as negative control). Our data strongly suggest that CK2-dependant phosphorylation of the Spt6 N-terminal region is involved in the modulation of histone H3 dynamics during transcription. Taken together, these data show that CK2 phosphorylation sites of the Spt6 N-terminal region are required for Spt6 chromatin functions.



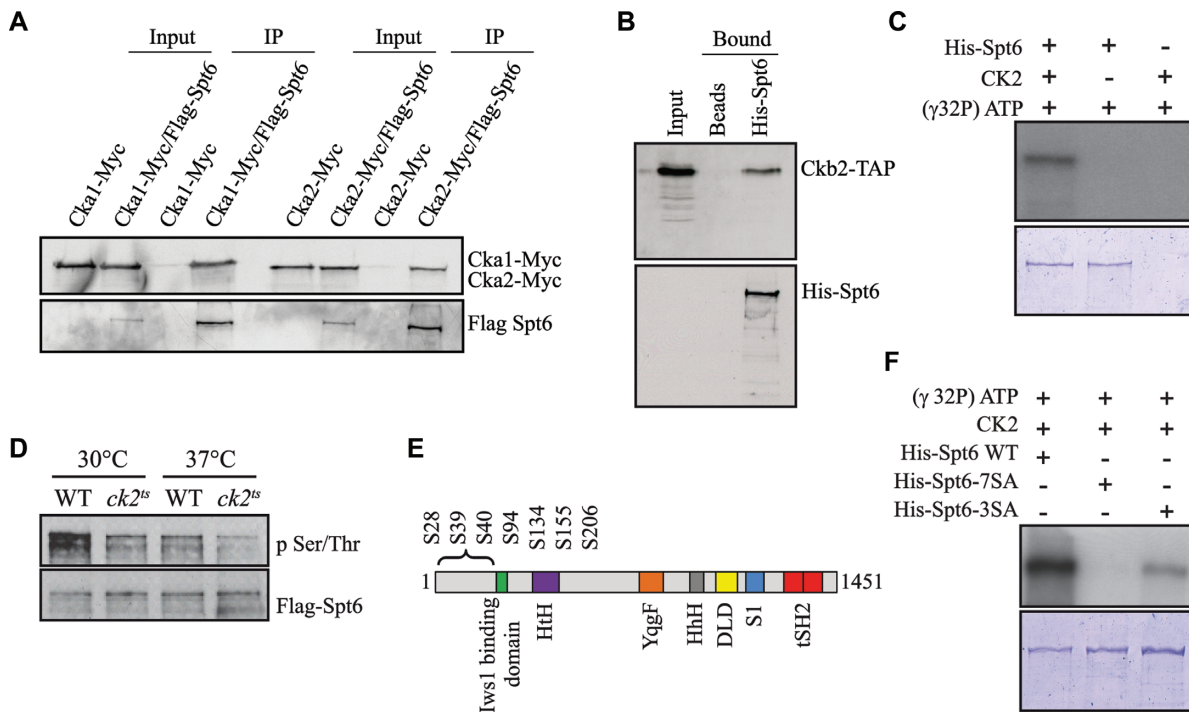


**Figure 3.** CK2 interacts with Spt6 and phosphorylates it *in vitro* and *in vivo*. (A) Spt6 interacts with different subunits of CK2 *in vivo*. Flag-Spt6 was immunopurified from strains expressing Cka1-Myc or Cka2-Myc. The purified samples were analyzed by western blot with antibodies against the Myc and Flag epitopes. A purification control was obtained using strains expressing untagged Spt6. (B) Spt6 interacts directly with CK2 *in vitro*. A His pull-down assay was performed using equal amounts of Ckb2-TAP purified from yeast and recombinant 6xHis-Spt6. Ni-NTA agar beads alone served as a control. (C) CK2 phosphorylates Spt6. *In vitro* phosphorylation assay of recombinant 6xHis-Spt6 with CK2 kinase purified from yeast. (D) Spt6 is phosphorylated *in vivo* in a CK2-dependent manner. Flag-Spt6 was immunopurified from WT and *ck2<sup>ts</sup>* strains grown at 30°C or at 37°C for 2 h. The purified samples were analyzed by western blot with antibodies against phosphoserine/phosphothreonine or Flag epitope. (E) Schematic representation of various domains of Spt6: potential CK2 target sites (S28, S39, S40, S94, S134, S155, S206) are all found in the N-terminal region. (F) The N-terminal phosphosites of Spt6 (S28, S39, S40, S94, S134, S155, S206) are required for the phosphorylation by yeast CK2. *In vitro* phosphorylation assay of recombinant 6xHis-Spt6 WT, and non-phosphorylatable mutants (6xHis-Spt6-3SA and -7SA) using CK2 kinase purified from yeast.

### Spt6 phosphorylation sites play an essential role in the global repression of antisense and cryptic transcription

To characterize further the role CK2-dependent Spt6 phosphorylation in transcription at high resolution, we performed strand-specific RNA-seq in mutant comparing WT to *spt6-7SA*. Approximately the same number of genes for which the sense transcripts levels were affected either positively or negatively (Figure 5A). Strikingly, *spt6-7SA* mutation led to the increase of antisense transcription in a significantly higher number of genes ( $P$  value <  $10e^{-70}$ , Ratio UP/Down 6:1). This is consistent with what we observed for the *ck2<sup>ts</sup>* mutant and suggests that Spt6 phosphorylation sites are required for the repression of antisense transcription. We next analyzed the data by comparing WT and *spt6-7SA* sense and antisense transcripts. Also, similar to what have been found in *ck2<sup>ts</sup>* cells, the Pearson correlation between WT and *spt6-7SA* data sets is reduced for the antisense transcripts (Figure 5B). The metagene analyses aligning sense and antisense transcripts to transcription start site further confirmed that the most striking effect of *spt6-7SA* mutation is to antisense transcription (Figure 5C and Supplementary Figure S7). Next, we confirmed our global data by testing antisense transcription in a specific locus. As for *ck2<sup>ts</sup>*, the RNA-seq analysis showed that *spt6-7SA* allele is associated with a signif-

icant induction of antisense transcription in *PHO84* locus (Figure 5D). We probed for the gene *YML122C* located upstream of *PHO84*. This gene is not transcriptionally active, no sense or antisense transcripts are observed unless antisense transcript initiates from *PHO84* coding region and extends into *YML122C* (Figure 5E). In *spt6-7SA* allele, a probe located in *YML122C* revealed a long antisense transcript (*PHO84-YML122C*) starting in *PHO84* and extending into *YML122C* (Figure 5E). Hence, these data indicate that CK2 phosphorylation sites in Spt6 are required for the repression of antisense transcription in yeast cells.

Spt6 is involved in the repression of global spurious transcription from cryptic promoters (12). As shown in Figure 4, mutations of CK2 phosphorylation sites lead to the derepression of the *FLO8* cryptic promoter suggesting that CK2 regulation of Spt6 may be involved in global control of sense cryptic transcripts level. To analyze the global role of CK2 regulation on cryptic transcripts, we measured the 3'/5' ratios in the *spt6-7SA* mutant for all genes and compared them to that of wild-type cells. In *spt6-7SA*, we found 563 genes with increased ratio suggesting that CK2 phosphorylation sites play an important role in the repression of cryptic transcription (Figure 5I, Supplementary Table S3). These data are reproducible as attested by the correlation shown in Supplementary Figure S8. To validate these results, we measured the 3'/5' ratio by RT-qPCR at

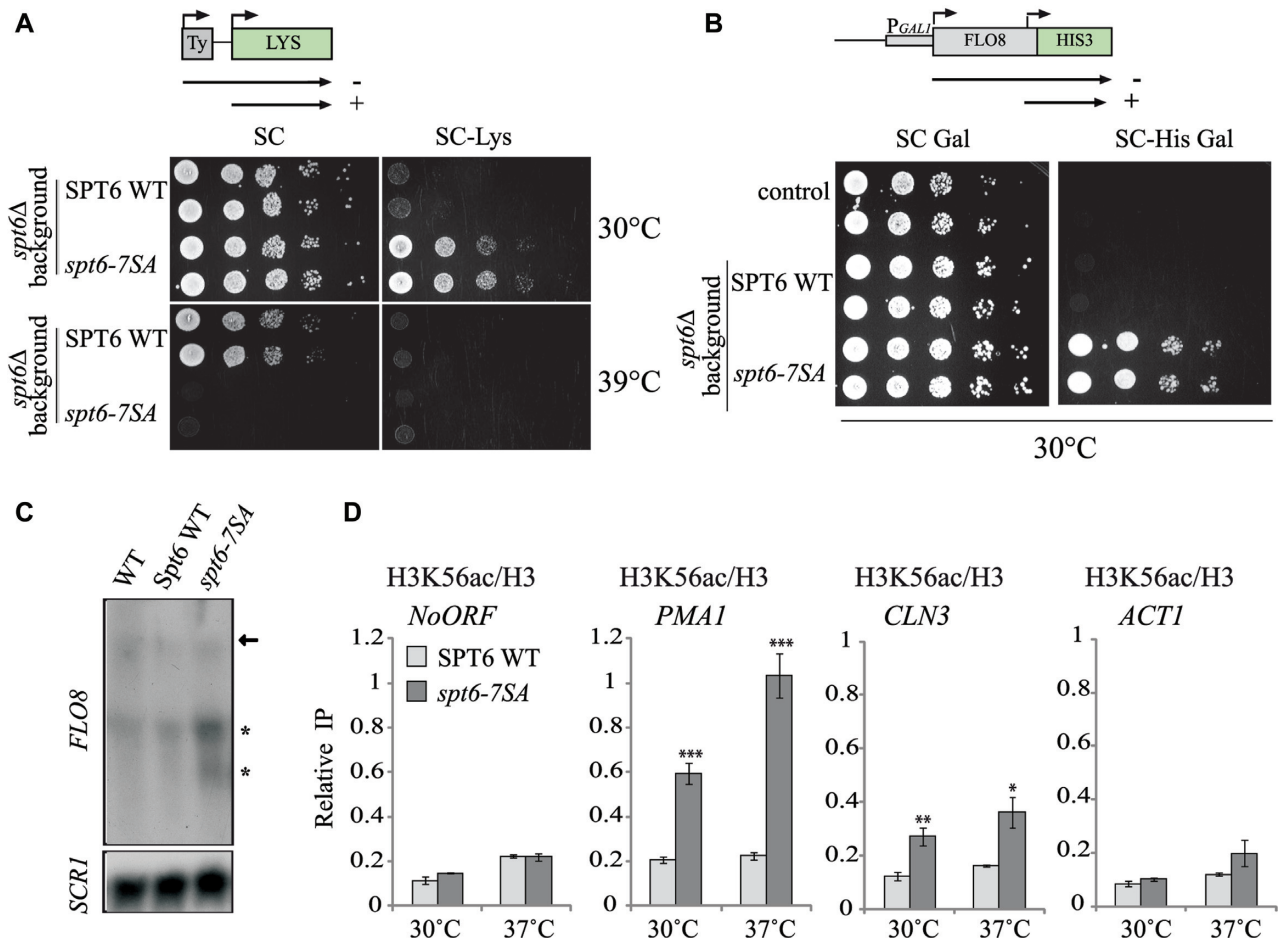


**Figure 4.** Phosphorylation by CK2 regulates Spt6 chromatin function. (A) Mutation of CK2 phosphosites in Spt6 leads to *spt*-phenotype. SPT6 WT and *spt6-7SA* (Serine to Alanine) strains containing the *Lys2-1288* SPT reporter allele were serially diluted and spotted on synthetic complete (SC) or SC medium lacking lysine (SC-Lys) at 30 or 39°C. The *spt6-7SA* allele is thermosensitive and has an *spt*-phenotype. (B) The *spt6-7SA* is not able to suppress spurious transcription from *FLO8* cryptic promoter. WT and *spt6*Δ strains expressing SPT6 WT or *spt6-7SA* containing *pGAL1-FLO8-HIS3* spurious transcription reporter were serially diluted and spotted on synthetic complete (SC) medium, or SC medium lacking histidine (SC-His) with Galactose as a carbon source. The *spt6-7SA* allele growth in absence of histidine indicates intragenic cryptic initiation within *FLO8* coding region. (C) The *spt6-7SA* mutant is associated with cryptic transcription. Cells expressing either SPT6 WT or *spt6-7SA* were grown in YPD at 37°C. Total RNA was isolated and analyzed by Northern blot with a probe specific for 3'-end of *FLO8*. *SCR1* served as loading control. (D) Replication-independent histone H3K56ac level is increased at coding regions of genes in *spt6-7SA* mutant. ChIP assays assessing the H3K56 acetylation level in G1-arrested cells expressing Spt6 or the mutated *spt6-7SA* version. Cells were G1-arrested and subsequently grown for 2 h at 30 or 37°C. The values shown represent the average and standard errors of three independent experiments measuring H3K56ac levels (IP/Input) relative to histone H3 occupancy (IP/Input). Coding regions of different genes were tested and NoORF is a non-transcribed control locus of chromosome V. (\*) *P* value < 0.05; (\*\*) *P* value < 0.01; (\*\*\*) *P* value < 0.001.

3 genes, *FLO8*, *SPO23* and *MAL33*, exhibiting 3' enrichment in *spt6-7SA* mutant RNA-seq signals (Figure 5F). Interestingly, as predicted by our RNA-seq analyses, *spt6-7SA* mutation is associated with a significant increase of 3'/5' transcripts ratio at *SPO23* or *MAL33* and a slight one at *FLO8* (Figure 5F). This effect is not observed in the negative controls *PMA1* and *FKS1*, confirming that CK2 regulation of Spt6 controls the cryptic transcripts levels at several genes identified by our analyses. Moreover, our RNA-seq 3'/5' ratios data also predicted the existence of cryptic transcripts produced from within *DDC1* 3'end but not in *SPB4* 3' end region. This was surprising because *SPB4* is a common model gene used in several studies of cryptic transcription and has been found to be affected in *ck2<sup>ts</sup>* cells (12). To further confirm our analyses, we probed the transcripts of *DDC1* and *SPB4* by Northern blot (Figure 5G). We

observed clear bands indicating short transcripts initiated from 3'end cryptic promoters of *FLO8* and *DDC1*, but not for *SPB4* as predicted by our analyses. Therefore, these data suggest significant but not complete overlap between *ck2<sup>ts</sup>* and *spt6-7SA* RNA-seq data sets. Together our observations indicate that CK2 phosphorylation of Spt6 is required for the repression of spurious transcription from cryptic promoters located within the coding regions of genes.

#### Spt6 phosphorylation mutants regulate cryptic sense and antisense transcription at promoters that are also affected by CK2

As suggested by our Northern blot experiments there are overlaps between *ck2<sup>ts</sup>* and *spt6-7SA* but also some differences as shown for *SPB4*. We wanted to address this question globally and know if the mutation of Spt6 phospho-

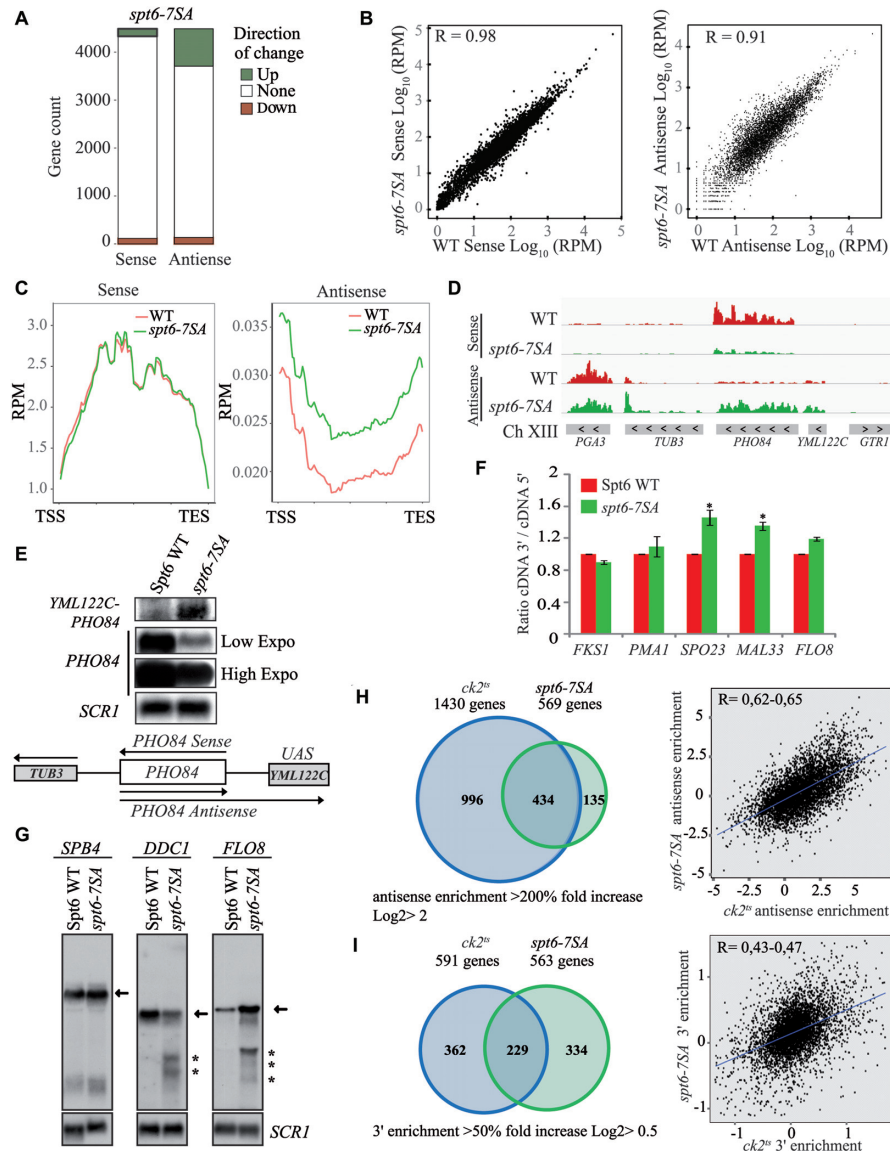


**Figure 5.** Spt6 phosphorylation regulates cryptic intragenic and antisense transcription. (A) Spt6 is required for the repression of antisense transcription in a high number of genes. A representation of genes count affected by at least two-fold either positively (green) or negatively (red) in *spt6-7SA* for sense or antisense transcripts levels. (B) The *spt6-7SA* antisense transcripts are less correlated with those of the wild-type (WT) strain. WT sense (left panel) or antisense (right panel)  $\log_{10}$  RPM scores for each transcription unit were plotted against *spt6-7SA* datasets. The Pearson correlation ( $R$  value) was calculated and is shown in each panel. (C) CK2 phosphorylation sites in SPT6 are required for the global repression of antisense transcription. Metagenic analysis showing WT and *spt6-7SA* RPM RNA-seq signals of the sense (left panel) or antisense (right panel) strands aligned over transcribed regions of genes. Transcription start site (TSS) and transcription end site (TES) are shown. A higher level of antisense transcription is observed in *spt6-7SA*. (D) Spt6 phosphosites are essential to the repression of antisense transcription in *PHO84* locus. A view of *PHO84* locus (chromosome XIII) sense and antisense strands transcripts data obtained by RNA-seq in WT (red) or *spt6-7SA* (green). (E) The CK2 phosphorylated residues play a crucial role in the repression of antisense transcription at *PHO84* locus. This observation was shown here by Northern blot analyses of *PHO84*-*YML122C* locus transcripts using different probes. *PHO84* probe was used to identify *PHO84* sense transcripts while *YML122C* probe was used specifically to follow the long antisense transcript that starts in *PHO84* and extends into *YML122C*. (F) Mutation of CK2 phosphorylated residues in Spt6 leads to 3'-enrichment of sense transcripts at *SPO23*, *MAL33* and *FLO8*. In this experiment, transcripts levels of the indicated genes were analyzed by RT-qPCR. The 5' and 3' regions of each gene were amplified and the values shown are 3'/5' ratios representing the average and standard errors of three independent experiments. (\*)  $P$  value < 0.05. (G) CK2-dependent phosphorylation of Spt6 is required for the repression of spurious transcription at *DDC1* and *SPB4*. Total RNA was isolated from cells after two hours of growth at 37 and analysed by northern blot with probes specific for 3'-end of *FLO8*, *DDC1*, and *SPB4*. *SCR1* was used as a loading control. Arrows indicate full-length RNA transcripts, and asterisks indicate short transcripts. (H) Significant overlap between *ck2<sup>ts</sup>* and *spt6-7SA* datasets for the genes with an increased antisense transcripts levels. The Venn diagram compares the number of genes with antisense enrichment in *ck2<sup>ts</sup>* and *spt6-7SA* mutants. The right panel is a correlation plot of antisense enrichment between *ck2<sup>ts</sup>* and *spt6-7SA* mutants. The *ck2<sup>ts</sup>* Antisense/Sense ratio relative to WT for each gene was plotted against *spt6-7SA* Antisense/Sense ratio relative to WT. The Pearson correlation coefficient ( $R$  value) was calculated and shows a positive and significant correlation between the two ratios. (I) Significant number of genes with predicted intragenic cryptic transcripts, identified by 3'-enrichment, in *ck2<sup>ts</sup>* overlap with those of *spt6-7SA* mutants. The Venn diagram compares the number of genes with 3' enrichment in *ck2<sup>ts</sup>* and *spt6-7SA* mutants. The right panel is a correlation plot of 3' enrichment between *ck2<sup>ts</sup>* and *spt6-7SA* mutants. The 3' enrichment of *ck2<sup>ts</sup>* for each gene was plotted against that of *spt6-7SA*. The Pearson correlation coefficient ( $R$  value) was calculated and shows a positive and significant correlation between the two data sets regarding cryptic transcripts.

rylation sites affects cryptic sense or antisense transcription at the same sites as CK2. We first compared *ck2<sup>ts</sup>* and *spt6-7SA* RNA-seq data sets for antisense transcripts and found positive and significant overlap between the two data sets (Figure 5H left panel and Supplementary Figure S9A). Moreover, we found positive correlation between the two data sets (Figure 5H right panel). Interestingly, we also observed the same type of relations between the two sets of data regarding the cryptic transcripts identified by the 3'/5' ratio (Figure 5I and Supplementary Figure S9B). The overlap was much higher than what would be expected by chance with *P* values less than  $8.529784e-67$  (Figure 5H and I; Supplementary Figure S9). Remarkably, 76% (434 out of 569) of the genes showing an increase of antisense transcription in *spt6-7SA* also produce higher antisense transcripts in *ck2<sup>ts</sup>* (Figure 5H). Together, these data establish a strong link between Spt6 phosphorylation and the global regulation of transcription accuracy by CK2. However, it must be noted that the group of CK2 genes producing pervasive antisense transcripts extends well beyond those affected in *spt6-7SA*. This suggests that, in addition to CK2–Spt6 pathway, this kinase may regulate additional sites independently of Spt6.

### CK2 phosphorylation sites are required for the stability of Spt6

The essential kinase CK2 regulates transcription accuracy possibly by modulating the activity of chromatin factors involved in the re-setting of the chromatin structure in the path of transcription. We have found that CK2 interacts and phosphorylates Spt6 which plays a major role in the refolding of nucleosomes in the body of genes. Our global data indicate that CK2 represses spurious transcription at many genes that are also affected by the loss of its phosphorylation sites in Spt6. These observations suggest that CK2 may influence, at least in part, the accuracy of transcription by phosphorylating Spt6 and thereby modulating its activity. Interestingly, by studying the effect of CK2 on Spt6/Iws1 complex, we observed that the level of the complex is significantly dependent on CK2 phosphorylation of Spt6 *in vitro* (data not shown). This effect is not observed *in vivo* (data not shown). However, we observed that CK2 depletion has a significant effect on total Spt6 protein level as indicated by Western blots shown in Figure 6A. This finding suggests a mechanism involving CK2 that regulates the cellular level of Spt6. We tested this by assessing the level of Spt6 in *spt6-7SA* cells. As shown in Figure 6B, mutation of CK2 phosphosites is clearly associated with a decreased level of Spt6. Interestingly, reducing the level of Spt6 just by 50% results in an impaired function, as shown in Supplementary Figure S10, supporting previous reports (46,65). The reduction of Spt6 level could be the consequence of either a defect in the production of the protein or an impaired stability. Because we did not observe a significant and a reproducible effect of CK2 on the production of *SPT6* transcripts by RT-QPCR (data not shown), we decided to test the second possibility by asking whether CK2 phosphorylation sites contributes to Spt6 stability. For that, Spt6 level was analyzed in wild-type and CK2 phosphosites mutant *spt6-7SA* cells grown in presence of cycloheximide, a protein synthesis inhibitor. As

shown in Figure 6C and Supplementary Figure S11, Spt6–7SA protein level decay was significantly faster than Spt6 WT decay. The half-life of Spt6–7SA was around two hours while that of Spt6 WT is approximately four hours. Importantly, expressing a version of Spt6 mimicking CK2 phosphorylation stabilized the protein and no significant decay was observed after six hours of cycloheximide treatment. This result indicates that CK2 phosphorylation sites play a major role in the maintenance of normal Spt6 level.

### Restoring Spt6 cellular level in CK2 depleted cells suppresses H3K56ac incorporation and spurious transcription

Our later findings regarding Spt6 stability bring about an interesting possibility involving CK2 regulation of histone H3 dynamics. Indeed, one can assume that if CK2 regulation modulates histone H3 dynamics by maintaining Spt6 cellular levels, then mimicking CK2 phosphorylation of Spt6 could affect this dynamic. To address this possibility, we analyzed the incorporation of new H3 in CK2 phosphosites mutants at the coding regions of several genes. The level of H3K56ac, a surrogate of new H3 incorporation, was assessed by ChIP assays in wild-type or *ck2<sup>ts</sup>* G1 arrested cells expressing either Spt6 WT or Spt6-7SD (Figure 6D). Interestingly, when the *ck2<sup>ts</sup>* cells express a wild-type Spt6, the H3K56ac level is increased at the coding regions of active genes at both permissive and restrictive temperatures. This shows higher replication-independent incorporation of newly synthesized H3 in *ck2<sup>ts</sup>* and indicates that in these regions, H3/H4 tetramers that are disrupted by elongating RNAP II are not recovered. Instead, in these locations, new H3/H4 tetramers are used to reassemble nucleosomes. Importantly, when *ck2<sup>ts</sup>* cells express a version of Spt6 that mimics CK2 phosphorylation, a clear suppression of the new H3 incorporation was observed at the coding regions of active genes. This indicates that CK2 function in the regulation of replication-independent H3/H4 dynamics is mediated by the phosphorylation of Spt6 and suggests that stable level of this factor plays a key role in this process. To further study the effect of Spt6 phosphorylation state on CK2 chromatin function, we asked if the suppression of histone H3 incorporation observed in *ck2<sup>ts</sup>* cells expressing a version mimicking CK2 phosphorylation is associated with a change in the spurious transcription. To this end, we analyzed by Northern blot the transcripts of *FLO8* gene. As shown in Figure 6E, in restrictive conditions, short transcripts are clearly observed in *ck2<sup>ts</sup>* cells expressing Spt6 WT or Spt6-7SA. Interestingly, *ck2<sup>ts</sup>* cells expressing Spt6-7SD display significantly less *FLO8* short transcripts indicating that a stable level of Spt6 suppresses spurious transcription from cryptic promoters in cells that are depleted in CK2 activity. Together, our findings demonstrate that CK2's function in suppression of spurious transcription is at least in part dependent on the regulation of Spt6 stability through its direct phosphorylation.

### CK2 and Spt6 phosphorylation sites are important for the efficient transcriptional response to environmental signals and stresses

CK2 has a widespread role in chromatin dynamics and the control of transcription accuracy without impacting tran-

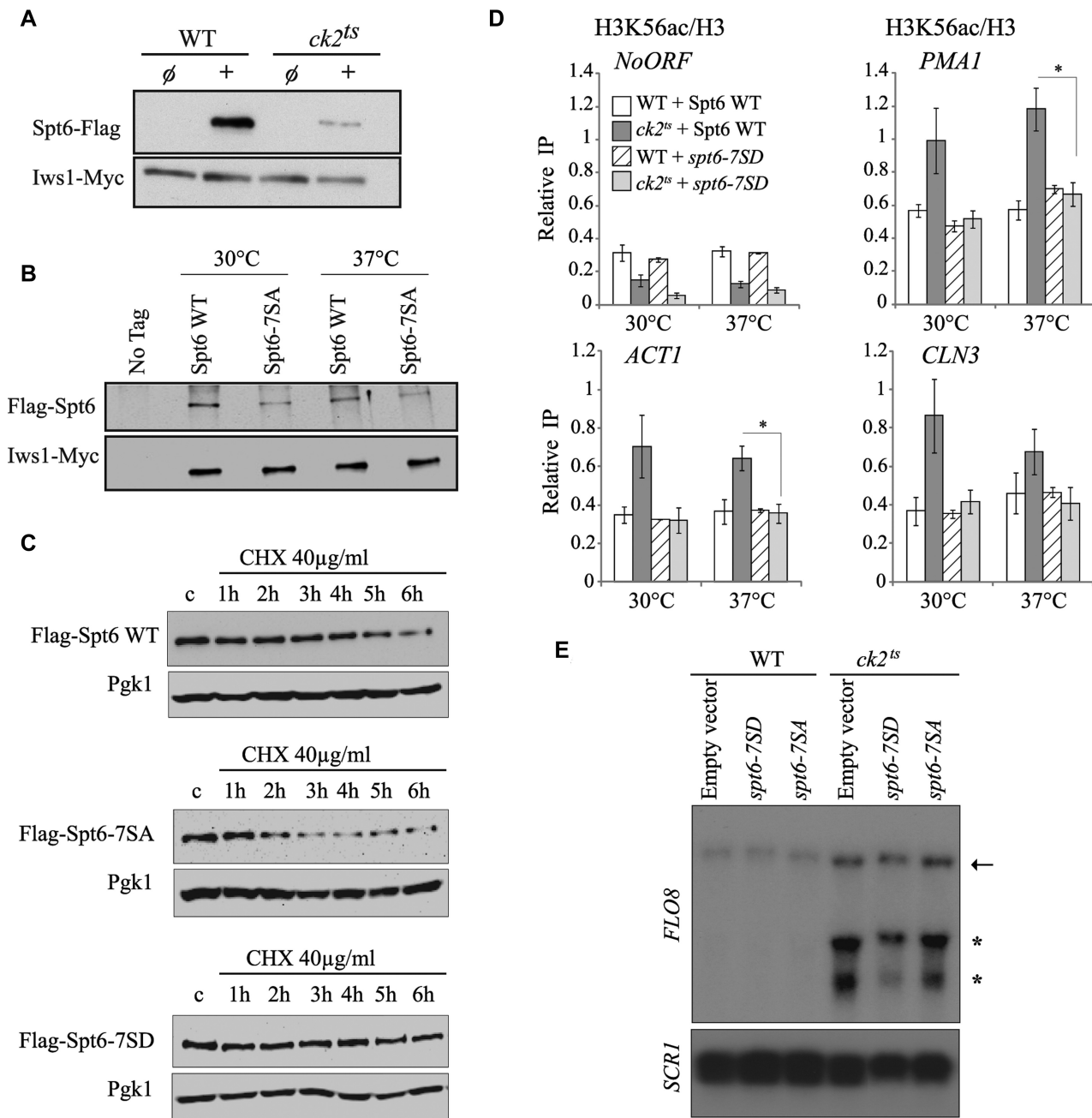


**Figure 6.** CK2 phosphorylation sites are critical for Spt6 stability and chromatin functions. (A) CK2 mutant is associated with a decrease of Spt6 cellular level. Flag-Spt6 and Iws1-Myc proteins were analyzed by western blots on total extracts from wild type (WT) or *ck2<sup>ts</sup>* heat-shocked cells using antibodies against Flag and Myc epitopes. (B) Mutation in CK2-dependent phosphosites leads to a decrease in Spt6 protein level. Flag-Spt6 and Iws1-Myc proteins were analyzed by western blots on chromatin extracts of cells expressing Flag-Spt6 or Flag-Spt6-7SA. (C) CK2-dependent phosphorylation of Spt6 is required for its stability. Flag-Spt6, Flag-Spt6-7SA (non-phosphorylatable) and Flag-Spt6-7SD (phosphomimic) proteins were analyzed by western blots on total extracts from heat-shocked cells treated for the time indicated with cycloheximide (CHX). Pgk1 was used as a loading control. Mutation of Spt6 phosphosites to alanine reduces its half-life while the change toward aspartic acid residues stabilizes this protein. (D) Spt6 phosphomimic mutant *spt6-7SD* suppresses the increased H3K56ac deposition observed in *ck2<sup>ts</sup>* mutant. ChIP assays assessing the H3K56 acetylation level in WT and *ck2<sup>ts</sup>* expressing Spt6 or Spt6-7SD. Cells were G1-arrested and subsequently grown for 1 h at 30 or 37°C. The values shown represent the average and standard errors of three independent experiments measuring H3K56ac levels (IP/Input) relative to histone H3 occupancy (IP/Input). Coding regions of different genes were tested and NoORF is a non-transcribed control locus of chromosome V. (\*) *P* value < 0.05. (E) Spt6 phosphomimic mutant *spt6-7SD* suppresses the cryptic transcription in *ck2<sup>ts</sup>* at *FLO8* gene. Cells expressing either Spt6-7SD or Spt6-7SA were grown in YPD at 30°C and then shifted 37°C for two hours. Total RNA was extracted and analyzed by northern blot using a specific *FLO8* 3' end probe. *SCRI* is a loading control.

scripts levels of most protein-encoding genes. Indeed, in standard conditions used in our study, the important production of spurious sense and antisense transcripts in CK2 depleted cells has only limited effects on gene expression. This surprising observation is however not restricted to CK2 and many chromatin modifiers have limited impact on gene expression (66). Interestingly, elegant studies showed that chromatin regulators have greater effect on the dynamics of gene expression than on the steady state transcription (66). Thus, it is possible that, similar to chromatin regulators, CK2 would modify the dynamics of transcriptional response. To test this, we first asked whether CK2 has a role in the dynamics of galactose induction at galactose responsive genes. In Figure 7A, a time-course of Rpb1 (a subunit of RNAP II) recruitment to *GAL2* gene is shown in both wild-type and *ck2<sup>ts</sup>* at permissive and restrictive temperatures. Interestingly, at both conditions, we observed a clear reduction of Rpb1 recruitment at *GAL2* while no such effect was observed at the constitutive gene *PMA1*. This defect was associated with a clear reduction of the *GAL2* mRNA production, indicating that CK2 affects the cellular response to carbon source shift (Figure 7B). Next, we wanted to know if CK2 phosphorylation sites in Spt6 are important for Rpb1 recruitment and *GAL2* transcriptional induction. Importantly, similar to *ck2<sup>ts</sup>* mutant, the recruitment of Rpb1 and the induction of *GAL2* induction are both impaired in *spt6-7SA* (Figure 7C and D). We further tested other transcriptional responses as histidine starvation by treating WT or mutant cells with 3-aminotriazole (3AT), a competitive inhibitor of His3. Both *ck2<sup>ts</sup>* and *spt6-7SA* mutations affected significantly this response regarding mRNA levels of different metabolic genes activated by amino-acid starvation such as *HIS4*, *ARG1* and *ATRI* (Figure 7E). We conclude that CK2 and the phosphorylation of Spt6 are required for the dynamic adaptation of cells to environmental changes and stresses.

## DISCUSSION

Proper refolding of chromatin during the course of transcription is tightly regulated. Defects in chromatin refolding have been linked to spurious transcription from cryptic promoters within the coding regions of different genes (12,14,22,23). Cryptic transcription is a widespread phenomenon in yeast, with many genes displaying such aberrant event. Importantly, it has also been reported in mammals (18,67). Different factors can suppress cryptic transcription, including histones, regulators of histone genes, chromatin remodeling factors, transcription elongation factors and histone chaperones (12,23,68). CK2's subunits have been associated with some of these factors. Indeed, subunits of CK2 have been found to be associated with different factors that modulate chromatin structure during transcription elongation (35,39,40). Previous studies suggested that CK2 may regulate chromatin structure (33,34,69). However, an exact mechanism of how such regulation operates remained largely elusive. Here we show, for the first time, clear and direct evidence of CK2's involvement in this process. Our data further support a physical and a functional link between CK2 and an essential HC, indicating a specific role of CK2 in chromatin structure dy-

namics. Furthermore, we identified a potential mechanism of how CK2 may regulate chromatin modulations associated with transcription elongation. By regulating this chromatin process, CK2 contributes directly to the suppression of cryptic intragenic sense and antisense transcription.

### CK2 controls the nature of nucleosomes in the 3' end of transcribed regions

During transcription elongation, nucleosomes are unfolded to allow the progression of the transcription machinery along DNA (3). Upon RNAP II passage, nucleosomes are refolded back, mainly by mechanisms that preserve the histone H3/H4 tetramers. These mechanisms involve histone H3/H4 chaperones such as Spt2 and Spt6 (19,20,57). In addition to nucleosomes refolding, histones are further modified by enzymes, including Set2, which incorporates methyl groups on lysine 36 of histone H3 (70). This modification is of great importance because it directs the deacetylation of histone H3/H4 tails and thereby stabilizes nucleosomes (22,70). Together, reassembly of nucleosomes and chemical modifications of histones are required for the repression of spurious transcription and the focusing of RNAP II on real promoters leading to production of transcripts translated into proteins. Our data show a key role of CK2 in chromatin remodeling in 3' end of coding regions. First, we found that CK2 activity is required for the control of H3K56 acetylation level in transcribed regions of several genes (Figure 1A). Second, we showed that new histone H3 incorporation in coding regions, a surrogate of nucleosomes turnover in these locations (5), is also tightly and globally controlled by CK2 (Figure 1C). Third, the high level of histone H3 exchange in CK2 depleted cells is specifically located in the 3' end regions of genes (Figure 1D). Thus, CK2 controls the nature of nucleosomes that are refolded back after the passage of RNAP II and this has important consequences. Indeed, a marked increase of replication-independent histone H3/H4 exchange means that those nucleosomes have different marks and may therefore display different properties. A high level of H3K56ac outside of S-phase indicates not only a higher histone H3/H4 turnover but also a higher general acetylation level of histone H3/H4 (22,70). As discussed above, acetylation of H3/H4 in coding region has a major impact on the role of the chromatin structure as barrier against RNAP II wrongful association in these locations. Our work shows that CK2 is required for the control of H3K56ac levels in coding regions and may influence indirectly other histone acetylation sites that could be important for the inhibition of cryptic promoters located within coding regions.

One important observation regarding CK2 and chromatin modulations, is that the high level of new histone H3 incorporation we observed in CK2 depleted cells is located in the 3' end regions of genes. These regions are typically enriched in histone H3K36me3 mark, which is known to play a major role in the inhibition of various cryptic promoters, and is involved in the control of histone H3 exchange at these locations (22). In addition, similar to a *set2* mutant, *ck2<sup>ts</sup>* did not affect the global levels of histones in coding regions (data not shown). Furthermore, Spt6/Iws1 complex is a key regulator of H3K36me3 and Set2 activity (62). Thus,

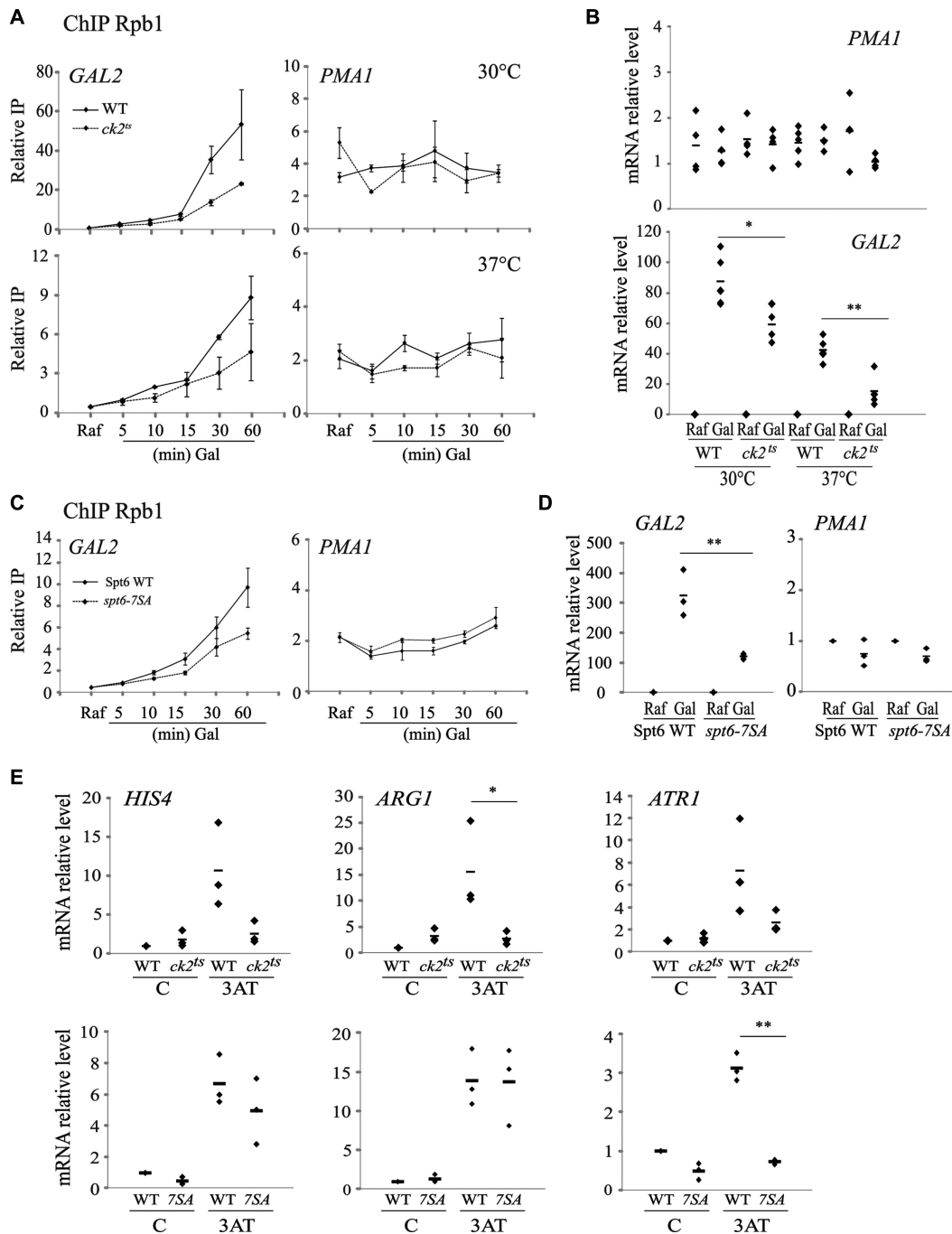


**Figure 7.** CK2 and its Spt6 phosphorylation sites are required for transcriptional response. (A) Rpb1 recruitment to galactose-inducible gene is affected by CK2 depletion. ChIP assays analysing Rpb1 recruitment to galactose inducible *GAL2* or to constitutive *PMA1* genes. Cells from WT or *ck2<sup>ts</sup>* strains were grown in raffinose to mid-log phase, galactose was added and cultures were shifted to the indicated temperatures (30°C: permissive or 37°C: non-permissive). The values shown represent the average and standard errors of three independent experiments measuring Rpb1 relative levels (IP/Input). (B) CK2 is required for the transcript level induction of the galactose responsive gene *GAL2*. RT-QPCR assessing transcripts levels of *GAL2* and *PMA1* upon galactose induction in WT and *ck2<sup>ts</sup>*. Total RNAs, extracted from cells treated as described in A, were analysed by RT-qPCR. (C) Rpb1 recruitment to galactose-inducible gene is affected by mutations of CK2 phosphosites in Spt6. ChIP assays analysing Rpb1 recruitment to galactose inducible *GAL2* or to constitutive *PMA1* genes. Cells expressing Spt6 or Spt6-7SA mutated version were grown in raffinose to mid-log phase and then galactose was added for the indicated time. The values shown represent the average and standard errors of three independent experiments measuring Rpb1 relative levels (IP/Input). (D) Spt6 phosphorylation sites are required for the transcript level induction of the galactose responsive gene *GAL2*. RT-QPCR assessing transcripts levels of *GAL2* and *PMA1* upon galactose induction in cells expressing WT Spt6 or Spt6-7SA. Total RNAs, extracted from cells treated as described in C, were analysed by RT-qPCR. (E) CK2 and its phosphorylation sites in Spt6 are required for the transcriptional response to histidine starvation. WT, *ck2<sup>ts</sup>* or cells expressing *spt6-7SA* were grown in SC-His medium, heat shocked at 37°C for 30 min and then treated with 40 mM 3-aminotriazole (3AT) for 1 h to induce amino acid starvation response. Total RNA was extracted, used to produce cDNA and quantified by QPCR at *HIS4*, *ARG1* and *ATR1* genes. For all RT-QPCR, the relative level is the ratio of the indicated RNA to the *SCRJ* transcript level. (\*) *P* value < 0.05; (\*\*) *P* value < 0.01; (\*\*\*) *P* value < 0.001.

CK2 has similarity towards Set2 on histone H3 exchange in 3' of coding regions, H3K56ac levels, histone H3 occupancy, and Spt6 function. Consequently, one could easily imagine that CK2 may influence chromatin modulations through the direct or indirect control of H3K36 methylation. Our data discard this possibility. First, in *ck2<sup>ts</sup>* cells, we did not observe an effect on H3K36me3 at all genes tested (Supplementary Figure S1C and data not shown). Second, the global level of these modifications was not significantly different in CK2 depleted cells from that of wild-type cells (Supplementary Figure S1B). Third, the recruitment of Set2 enzyme was directly assessed by ChIP assays in *ck2<sup>ts</sup>* cells and no significant change has been observed (data not shown). Therefore, we conclude that CK2 controls the chromatin dynamics in the coding regions through one or more pathway(s) and none of these include Set2 and H3K36me3.

### CK2-mediated phosphorylation of Spt6 modulates chromatin in transcribed regions

Several new observations made in this work point toward a direct regulation of one of the main histone chaperone involved in chromatin modulations during transcription elongation. Indeed, we found that Spt6 is phosphorylated on several residues by CK2 both *in vivo* and *in vitro* (Figure 3). These phosphosites have an important impact on the function of Spt6 and their mutation leads to defects in the suppression of Ty transcription (Figure 4). In addition, they are required for the control of H3K56ac levels and recycling of H3/H4 tetramers in coding regions. Consequently, the Spt6 version mutated in CK2 phosphosites cannot achieve the repression of spurious transcription, as shown by reporter assay, Northern blot and RNA-seq data (Figures 4 and 5). Importantly, we demonstrated that mimicking CK2 phosphorylation results in rescue of *ck2<sup>ts</sup>* phenotypes on both histone H3K56ac and spurious transcription (Figure 6C and D). Thus, we feel confident that a significant part of CK2 regulation proceeds through Spt6 phosphorylation. This is especially the case for histone H3 dynamics, given the fact that the expression of an Spt6 version mimicking CK2 phosphorylation in *ck2<sup>ts</sup>* mutants leads to a complete repression of histone H3K56ac increased incorporation in the tested coding regions (Figure 6D). However, CK2 control of cryptic sense and antisense transcription extends beyond the role of Spt6. Indeed, despite good overlap between *ck2<sup>ts</sup>* and *spt6-7SA* data sets regarding genes producing intragenic or antisense transcripts, differences do exist. This is well illustrated by the comparison of *ck2<sup>ts</sup>* and *spt6-7SA* genes that were affected for antisense transcripts. We observed that almost 80% of genes affected in *spt6-7SA* also produce antisense transcripts in *ck2<sup>ts</sup>*. However, CK2 mutant affects many more genes and only 32% are common with *spt6-7SA*. Several possibilities could explain these observations. In our experimental conditions, *ck2<sup>ts</sup>* could simply have indirect effects that would result in more drastic phenotypes. Alternatively, CK2 could regulate different factor(s) that would modulate directly the initiation from different cryptic sense or antisense promoters. Interestingly, CK2 has been directly linked with FACT and PAF elongation complexes and H2B ubiquitylation (33,35,39) which

were associated with spurious transcription and chromatin reassembly (71,72). The existence of such an alternative pathway is supported by the partial suppression of CK2 spurious transcription when *Spt6-7SD* is expressed.

Finally, we should mention that Spt6 partner, Iws1, is a potential target of CK2 (35). In addition to Spt6, CK2 may regulate the other subunit of the Spt6/Iws1 complex and this regulation could have a significant role in the overall control of transcription accuracy. Thus, it would be interesting to test if CK2 modulates Iws1 and how this potential regulation affects the chromatin function of Spt6/Iws1 complex and spurious transcription. In any ways, CK2 regulates Spt6 function by maintaining its cellular levels. This has direct consequences on histone H3/H4 dynamics in coding region and thereby transcription accuracy.

### CK2 may help RNAP II to focus on real promoters and therefore allows optimal cell response to environmental challenges

In cells depleted of CK2 activity, we measured high levels of cryptic sense and antisense transcripts (Figure 2). It is likely that this spurious transcription would have a major impact on *bona fide* genes transcription. Indeed, an increasing number of studies in various organisms show that non-coding RNA and their transcription directly and indirectly regulate the transcription of genes (15,17,73,74). Our data do not allow us to draw clear conclusions on steady state transcripts levels of genes (Figure 2C). One could expect that transcription from a cryptic promoter driving either sense or antisense transcription would impact and compete with the normal canonical promoter. We assessed this possibility by analyzing the link between changes in the transcription of *bona fide* genes and the presence of spurious transcription in these genes. Unfortunately, we did not observe a significant correlation between the normal transcript variation and production of spurious transcription (data not shown). Importantly, this is consistent with previous observations made on *spt6-1004* mutant cells in which massive spurious transcription has been observed (12,27). In this mutant, no significant correlation between spurious transcription and transcription from canonical promoters has been reported (27). It was proposed that absence of obvious link may be caused by *spt6-1004s'* drastic effects on chromatin structure including massive loss of nucleosomes (25). Importantly, in our experimental conditions, no such effect has been observed in CK2 depleted cells and histone H3 levels taken as an assessment of nucleosomes occupancy was not changed (data not shown). Thus, in the light of our data, it seems unlikely that mutant with less drastic effect would allow us to uncover or analyze better a potential relationship between spurious and canonical transcription. Hence, the question of the spurious transcription effect on the *bona fide* gene expression remains unanswered. Two possibilities explaining the transcriptional role of CK2 may be discussed. First, cryptic transcription could have no impact on gene expression. This would be consistent with many observations regarding the phenotypes of mutants that produce spurious transcripts without a significant outcome on transcription from regular promoters. Indeed, mutants of the HCs Spt2 or the methyltransferase Set2 are associated with cryptic transcription that has virtually no impact on their growth



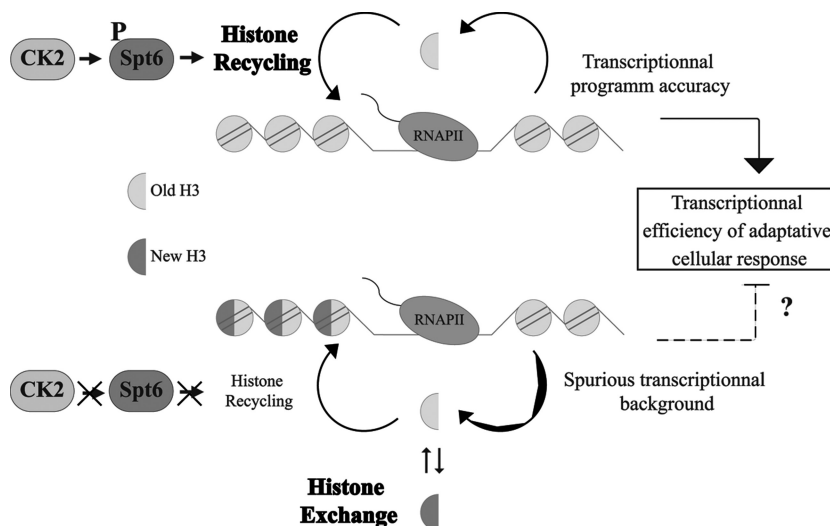


**Figure 8.** Mechanism of chromatin regulation by CK2. In presence of CK2 activity, Spt6 is phosphorylated and its level is maintained. This allows the proper recycling of histones H3/H4 tetramers and ensures the accuracy of transcription by repressing spurious transcription. Altogether, these functions could lead to the efficiency of the transcriptional response.

fitness or even global gene expression (75,76). However, it is important to note that despite their importance, many chromatin factors mutants have mild effects on global gene expression. Presumably, this is due to homeostatic mechanisms that compensate for the loss of chromatin regulators (66).

Interestingly, looking at model genes, such as *PHO5*, suggest a second possibility that may explain the potential transcription role of CK2. Indeed, in steady state standard conditions, *PHO5* transcription is not generally affected by the loss of many chromatin factors. This is however not the case when cells are challenged to produce rapidly the Pho5 alkaline phosphatase (77,78). Therefore, in the case of CK2, we reasoned that CK2 repression of spurious transcription may be important for the response to environmental challenges. As shown in our study, all stresses conditions tested in *ck2<sup>ts</sup>* mutant led to the observation of a defect in the transcriptional response (Figure 7). Moreover, this was also observed in the Spt6 phosphosite mutant (Figure 7). Our observation is consistent with elegant global studies showing that chromatin factors have only mild effects on steady state transcription, but are severely impaired in transcriptional stress response (66). Without excluding other possibilities, such as a role of CK2/Spt6 phosphorylation in the transcriptional induction itself, a disturbed chromatin dynamics and the induction of spurious transcription may affect transcriptional response. In summary, our study shows a new role of CK2 in the regulation of histone H3/H4 dynamics through the phosphorylation of the HC Spt6. We propose a mechanism (see model Figure 8) where CK2 phosphorylates the Spt6 N-terminal domain and these modifications stabilize Spt6. Consequently, this HC recycles H3/H4 tetramers and nucleosomes are adequately refolded back. Finally, we suggest that CK2 modulates other substrate that collaborate to the inhibition of spurious transcription. Future studies focused on these factors should give us a full picture on how this conserved kinase controls the accuracy of transcription.

## DATA AVAILABILITY

The genomic datasets from this study have been deposited in NCBI's Gene Expression Omnibus (GEO) database under accession number GSE109080.

## SUPPLEMENTARY DATA

Supplementary Data are available at NAR Online.

## ACKNOWLEDGEMENTS

We thank S. Bilodeau and S. Hussein for the critical review of the manuscript.

## FUNDING

CIHR [PJT-148780]; A. Nourani holds a Canadian Chair research. Funding for open access charge: CIHR. *Conflict of interest statement.* None declared.

## REFERENCES

- Kornberg, R.D. (1977) Structure of chromatin. *Ann. Rev. Biochem.*, **46**, 931–954.
- Selth, L.A., Sigurdsson, S. and Svejstrup, J.Q. (2010) Transcript elongation by RNA polymerase II. *Ann. Rev. Biochem.*, **79**, 271–293.
- Venkatesh, S. and Workman, J.L. (2015) Histone exchange, chromatin structure and the regulation of transcription. *Nat. Rev. Mol. Cell Biol.*, **16**, 178.
- Kulaeva, O.I., Hsieh, F.K., Chang, H.W., Luse, D.S. and Studitsky, V.M. (2013) Mechanism of transcription through a nucleosome by RNA polymerase II. *Biochim. Biophys. Acta*, **1829**, 76–83.
- Rando, O.J. and Winston, F. (2012) Chromatin and transcription in yeast. *Genetics*, **190**, 351–387.
- Gaykalova, D.A., Kulaeva, O.I., Volokh, O., Shaytan, A.K., Hsieh, F.-K., Kirpichnikov, M.P., Sokolova, O.S. and Studitsky, V.M. (2015) Structural analysis of nucleosomal barrier to transcription. *Proc. Natl. Acad. Sci. U.S.A.*, **112**, E5787–E5795.
- Avvakumov, N., Nourani, A. and Côté, J. (2011) Histone chaperones: modulators of chromatin marks. *Mol. Cell*, **41**, 502–514.

8. Gurard-Levin, Z.A., Quivy, J.-P. and Almouzni, G. (2014) Histone Chaperones: Assisting histone traffic and nucleosome dynamics. *Annu. Rev. Biochem.*, **83**, 487–517.
9. Hammond, C.M., Strømme, C.B., Huang, H., Patel, D.J. and Groth, A. (2017) Histone chaperone networks shaping chromatin function. *Nat. Rev. Mol. Cell Biol.*, **18**, 141–158.
10. Kireeva, M.L., Walter, W., Tchernajenko, V., Bondarenko, V., Kashlev, M. and Studitsky, V.M. (2002) Nucleosome remodeling induced by RNA polymerase II: loss of the H2A/H2B dimer during transcription. *Mol. Cell*, **9**, 541–552.
11. Studitsky, V.M., Walter, W., Kireeva, M., Kashlev, M. and Felsenfeld, G. (2004) Chromatin remodeling by RNA polymerases. *Trends Biochem. Sci.*, **29**, 127–135.
12. Chung, V., Chua, G., Batada, N.N., Landry, C.R., Michnick, S.W., Hughes, T.R. and Winston, F. (2008) Chromatin- and transcription-related factors repress transcription from within coding regions throughout the *Saccharomyces cerevisiae* genome. *PLoS Biol.*, **6**, 2550–2562.
13. DeGennaro, C.M., Alver, B.H., Marguerat, S., Stepanova, E., Davis, C.P., Bahler, J., Park, P.J. and Winston, F. (2013) Spt6 regulates intragenic and antisense transcription, nucleosome positioning, and histone modifications genome-wide in fission yeast. *Mol. Cell Biol.*, **33**, 4779–4792.
14. Shetty, A., Kallgren, S.P., Demel, C., Maier, K.C., Spatt, D., Alver, B.H., Cramer, P., Park, P.J. and Winston, F. (2017) Spt5 plays vital roles in the control of sense and antisense transcription elongation. *Mol. Cell*, **66**, 77–88.
15. Camblong, J., Beyrouthy, N., Guffanti, E., Schlaepfer, G., Steinmetz, L.M. and Stutz, F. (2009) Trans-acting antisense RNAs mediate transcriptional gene cosuppression in *S. cerevisiae*. *Genes Dev.*, **23**, 1534–1545.
16. Gérard, A., Ségéral, E., Naughtin, M., Abdouni, A., Charmeteau, B., Cheyner, R., Rain, J.-C. and Emiliani, S. (2015) The integrase cofactor LEDGF/p75 associates with Iws1 and Spt6 for postintegration silencing of HIV-1 gene expression in latently infected cells. *Cell Host Microbe*, **17**, 107–117.
17. Lenstra, T.L., Coulon, A., Chow, C.C., Larson, D.R., Lenstra, T.L., Coulon, A., Chow, C.C. and Larson, D.R. (2015) Single-Molecule imaging reveals a switch between spurious and functional ncRNA transcription. *Mol. Cell*, **60**, 597–610.
18. Xie, L., Pelz, C., Wang, W., Bashar, A., Varlamova, O., Shadle, S. and Impey, S. (2011) KDM5B regulates embryonic stem cell self-renewal and represses cryptic intragenic transcription. *EMBO J.*, **30**, 1473–1484.
19. Chen, S., Rufiange, A., Huang, H., Rajashankar, K.R., Nourani, A. and Patel, D.J. (2015) Structure-function studies of histone H3/H4 tetramer maintenance during transcription by chaperone Spt2. *Genes Dev.*, **29**, 1326–1340.
20. Kato, H., Okazaki, K., Iida, T., Nakayama, J.-I., Murakami, Y. and Urano, T. (2013) Spt6 prevents transcription-coupled loss of posttranslationally modified histone H3. *Scientific Rep.*, **3**, 2186.
21. Rufiange, A., Jacques, P.-É., Bhat, W., Robert, F. and Nourani, A. (2007) Genome-Wide Replication-Independent histone H3 exchange occurs predominantly at promoters and implicates H3 K56 acetylation and Asf1. *Mol. Cell*, **27**, 393–405.
22. Venkatesh, S., Smolle, M., Li, H., Gogol, M.M., Saint, M., Kumar, S., Natarajan, K. and Workman, J.L. (2012) Set2 methylation of histone H3 lysine 36 suppresses histone exchange on transcribed genes. *Nature*, **489**, 452–455.
23. Jeronimo, C., Watanabe, S., Kaplan, C.D., Peterson, C.L. and Robert, F. (2015) The histone chaperones FACT and Spt6 restrict H2A.Z from intragenic locations. *Mol. Cell*, **58**, 1113–1123.
24. Bortvin, A. and Winston, F. (1996) Evidence that Spt6p controls chromatin structure by a direct interaction with histones. *Science*, **272**, 1473–1476.
25. Ivanovska, I., Jacques, P.-É., Rando, O.J., Robert, F. and Winston, F. (2011) Control of chromatin structure by spt6: different consequences in coding and regulatory regions. *Mol. Cell Biol.*, **31**, 531–541.
26. Kaplan, C.D., Laprade, L. and Winston, F. (2003) Transcription elongation factors repress transcription initiation from cryptic sites. *Science*, **301**, 1096–1099.
27. Uwimana, N., Collin, P., Jeronimo, C., Haibe-Kains, B. and Robert, F. (2017) Bidirectional terminators in *Saccharomyces cerevisiae* prevent cryptic transcription from invading neighboring genes. *Nucleic Acids Res.*, **45**, 6417–6426.
28. Bhat, W., Boutin, G., Rufiange, A. and Nourani, A. (2013) Casein kinase 2 associates with the yeast chromatin reassembly factor Spt2/Sin1 to regulate its function in the repression of spurious transcription. *Mol. Cell Biol.*, **33**, 4198–4211.
29. Meggio, F. and Pinna, L.A. (2003) One-thousand-and-one substrates of protein kinase CK2? *FASEB J.*, **17**, 349–368.
30. St-Denis, N.A. and Litchfield, D.W. (2009) From birth to death: The role of protein kinase CK2 in the regulation of cell proliferation and survival. *Cell. Mol. Life Sci.*, **66**, 1817–1829.
31. Deplus, R., Blanchon, L., Rajavelu, A., Boukaba, A., Defrance, M., Luciani, J., Rothé, F., Dedeurwaerder, S., Denis, H., Brinkman, A.B. et al. (2014) Regulation of DNA methylation patterns by CK2-mediated phosphorylation of Dnmt3a. *Cell Rep.*, **8**, 743–753.
32. Wu, S.Y., Lee, A.Y., Lai, H.T., Zhang, H. and Chiang, C.M. (2013) Phospho switch triggers brd4 chromatin binding and activator recruitment for gene-specific targeting. *Mol. Cell*, **49**, 843–857.
33. Basnet, H., Su, X.B., Tan, Y., Meisenhelder, J., Merkurjev, D., Ohgi, K.A., Hunter, T., Pillus, L. and Rosenfeld, M.G. (2014) Tyrosine phosphorylation of histone H2A by CK2 regulates transcriptional elongation. *Nature*, **516**, 267–271.
34. Calvert, M.E.K., Keck, K.M., Ptak, C., Shabanowitz, J., Hunt, D.F. and Pemberton, L.F. (2008) Phosphorylation by casein kinase 2 regulates Nap1 localization and function. *Mol. Cell Biol.*, **28**, 1313–1325.
35. Krogan, N.J., Kim, M., Ahn, S.H., Zhong, G., Kobor, M.S., Cagney, G., Emili, A., Shilatifard, A., Buratowski, S. and Greenblatt, J.F. (2002) RNA polymerase II elongation factors of *saccharomyces cerevisiae*: a targeted proteomics approach. *Mol. Cell Biol.*, **22**, 6979–6992.
36. Dastidar, E.G., Dayer, G., Holland, Z.M., Dorin-Semblat, D., Claes, A., Chene, A., Sharma, A., Hamelin, R., Moniatte, M., Lopez-Rubio, J.-J. et al. (2012) Involvement of plasmodium falciparum protein kinase CK2 in the chromatin assembly pathway. *BMC Biol.*, **10**, 5.
37. Bouazoune, K. and Brehm, A. (2005) dMi-2 chromatin binding and remodeling activities are regulated by dCK2 phosphorylation. *J. Biol. Chem.*, **280**, 41912–41920.
38. Li, Y., Keller, D.M., Scott, J.D. and Lu, H. (2005) CK2 phosphorylates SSRP1 and inhibits its DNA-binding activity. *J. Biol. Chem.*, **280**, 11869–11875.
39. Bedard, L.G., Dronamraju, R., Kerschner, J.L., Hunter, G.O., Axley, E.D., Boyd, A.K., Strahl, B.D. and Mosley, A.L. (2016) Quantitative analysis of dynamic protein interactions during transcription reveals a role for casein kinase II in Polymerase-associated Factor (PAF) complex phosphorylation and regulation of histone H2B monoubiquitylation. *J. Biol. Chem.*, **291**, 13410–13420.
40. Gavin, A.-C., Bösch, M., Krause, R., Grandi, P., Marzioch, M., Bauer, A., Schultz, J., Rick, J.M., Michon, A.-M., Cruciat, C.-M. et al. (2002) Functional organization of the yeast proteome by systematic analysis of protein complexes. *Nature*, **415**, 141–147.
41. Winston, F., Dollard, C. and Ricupero-Hovasse, S.L. (1995) Construction of a set of convenient *saccharomyces cerevisiae* strains that are isogenic to S288C. *Yeast*, **11**, 53–55.
42. Longtine, M.S., McKenzie, A., Demarini, D.J., Shah, N.G., Wach, A., Brachat, A., Philippsen, P. and Pringle, J.R. (1998) Additional modules for versatile and economical PCR-based gene deletion and modification in *Saccharomyces cerevisiae*. *Yeast*, **14**, 953–961.
43. Puig, O., Caspary, F., Rigaut, G., Rutz, B., Bouveret, E., Bragado-Nilsson, E., Wilm, M. and Séraphin, B. (2001) The tandem affinity purification (TAP) method: a general procedure of protein complex purification. *Methods*, **24**, 218–229.
44. Goldstein, A.L. and McCusker, J.H. (1999) Three new dominant drug resistance cassettes for gene disruption in *Saccharomyces cerevisiae* - Goldstein - 1999 - Yeast - Wiley Online Library. *Yeast*, **15**, 1541–1553.
45. Kitazono, A.A., Tobe, B.T.D., Kalton, H., Diamant, N. and Kron, S.J. (2002) Marker-fusion PCR for one-step mutagenesis of essential genes in yeast. *Yeast*, **19**, 141–149.
46. Clark-Adams, C.D. and Winston, F. (1987) The SPT6 gene is essential for growth and is required for delta-mediated transcription in *Saccharomyces cerevisiae*. *Mol. Cell Biol.*, **7**, 679–686.

47. Rose, M.D., Novick, P., Thomas, J.H., Botstein, D. and Fink, G.R. (1987) A *Saccharomyces cerevisiae* genomic plasmid bank based on a centromere-containing shuttle vector. *Gene*, **60**, 237–243.
48. Nourani, A., Doyon, Y., Utley, R.T., Lane, W.S., Côté, J. and Allard, P. (2001) Role of an ING1 growth regulator in transcriptional activation and targeted histone acetylation by the NuA4 complex: role of an ING1 growth regulator in transcriptional activation and targeted histone acetylation by the NuA4 complex. *Mol. Cell. Biol.*, **21**, 7629–7640.
49. Bolger, A.M., Lohse, M. and Usadel, B. (2014) Trimmomatic: a flexible trimmer for Illumina sequence data. *Bioinformatics*, **30**, 2114–2120.
50. Li, H. and Durbin, R. (2009) Fast and accurate short read alignment with Burrows-Wheeler transform. *Bioinformatics*, **25**, 1754–1760.
51. Anders, S. and Huber, W. (2010) Differential expression analysis for sequence count data. *Genome Biol.*, **11**, R106.
52. Li, H., Handsaker, B., Wysoker, A., Fennell, T., Ruan, J., Homer, N., Marth, G., Abecasis, G. and Durbin, R. (2009) The Sequence Alignment/Map format and SAMtools. *Bioinformatics*, **25**, 2078–2079.
53. Ramirez, F., Ryan, D.P., Grüning, B., Bhardwaj, V., Kilpert, F., Richter, A.S., Heyne, S., Dündar, F. and Manke, T. (2016) deepTools2: a next generation web server for deep-sequencing data analysis. *Nucleic Acids Res.*, **44**, W160–W165.
54. Langmead, B., Trapnell, C., Pop, M. and Salzberg, S.L. (2009) Ultrafast and memory-efficient alignment of short DNA sequences to the human genome. *Genome Biol.*, **10**, R25.
55. Quinlan, A.R. and Hall, I.M. (2010) BEDTools: a flexible suite of utilities for comparing genomic features. *Bioinformatics*, **26**, 841–842.
56. Shen, L., Shao, N., Liu, X. and Nestler, E. (2014) ngs.plot: Quick mining and visualization of next-generation sequencing data by integrating genomic databases. *BMC Genomics*, **15**, 284–284.
57. Ferrari, P. and Strubin, M. (2015) Uncoupling histone turnover from transcription-associated histone H3 modifications. *Nucleic Acids Res.*, **43**, 3972–3985.
58. Dion, M.F., Kaplan, T., Kim, M., Buratowski, S., Friedman, N. and Rando, O.J. (2007) Dynamics of Replication-Independent histone turnover in budding yeast. *Science*, **315**, 1405–1408.
59. Cambong, J., Iglesias, N., Fickentscher, C., Dieppo, G. and Stutz, F. (2007) Antisense RNA stabilization induces transcriptional gene silencing via histone deacetylation in *S. cerevisiae*. *Cell*, **131**, 706–717.
60. van Bakel, H., Tsui, K., Gebbia, M., Mnaimneh, S., Hughes, T.R. and Nislow, C. (2013) A compendium of nucleosome and transcript profiles reveals determinants of chromatin architecture and transcription. *PLoS Genet.*, **9**, e1003479.
61. Carrozza, M.J., Li, B., Florens, L., Suganuma, T., Swanson, S.K., Lee, K.K., Shia, W.-J., Anderson, S., Yates, J., Washburn, M.P. et al. (2005) Histone H3 methylation by Set2 directs deacetylation of coding regions by Rpd3S to suppress spurious intragenic transcription. *Cell*, **123**, 581–592.
62. Yoh, S.M., Lucas, J.S. and Jones, K.A. (2008) The Iws1: Spt6: CTD complex controls cotranscriptional mRNA biosynthesis and HYPB / Set2-mediated histone H3K36 methylation. *Genes Dev.*, **22**, 3422–3434.
63. Albuquerque, C.P., Smolka, M.B., Payne, S.H., Bafna, V., Eng, J. and Zhou, H. (2008) A multidimensional chromatography technology for in-depth phosphoproteome analysis. *Mol. Cell. Proteomics*, **7**, 1389–1396.
64. Li, X., Gerber, S.A., Rudner, A.D., Beausoleil, S.A., Haas, W., Villén, J., Elias, J.E. and Gygi, S.P. (2007) Large-Scale phosphorylation analysis of  $\alpha$ -Factor-Arrested *Saccharomyces cerevisiae*. *J. Proteome Res.*, **6**, 1190–1197.
65. McCullough, L., Connell, Z., Petersen, C. and Formosa, T. (2015) The abundant histone chaperones Spt6 and FACT collaborate to assemble, inspect, and maintain chromatin structure in *Saccharomyces cerevisiae*. *Genetics*, **201**, 1030–1045.
66. Weiner, A., Chen, H.V., Liu, C.L., Rahat, A., Klien, A., Soares, L., Gudipati, M., Pfeffner, J., Regev, A., Buratowski, S. et al. (2012) Systematic dissection of roles for chromatin regulators in a yeast stress response. *PLoS Biol.*, **10**, e1001369.
67. Hainer, S.J., Gu, W., Carone, B.R., Landry, B.D., Rando, O.J., Mello, C.C. and Fazio, T.G. (2015) Suppression of pervasive noncoding transcription in embryonic stem cells by esBAF. *Genes Dev.*, **29**, 362–378.
68. Smolle, M., Venkatesh, S., Gogol, M.M., Li, H., Zhang, Y., Florens, L., Washburn, M.P. and Workman, J.L. (2012) Chromatin remodelers Isw1 and Chd1 maintain chromatin structure during transcription by preventing histone exchange. *Nat. Struct. Mol. Biol.*, **19**, 884–892.
69. Barz, T. (2003) Genome-wide expression screens indicate a global role for protein kinase CK2 in chromatin remodeling. *J. Cell Sci.*, **116**, 1563–1577.
70. Li, B., Gogol, M., Carey, M., Pattenden, S.G., Seidel, C. and Workman, J.L. (2007) Infrequently transcribed long genes depend on the Set2/Rpd3S pathway for accurate transcription. *Genes Dev.*, **21**, 1422–1430.
71. Chu, Y., Simic, R., Warner, M.H., Arndt, K.M. and Prelich, G. (2007) Regulation of histone modification and cryptic transcription by the Bur1 and Paf1 complexes. *EMBO J.*, **26**, 4646–4656.
72. Fleming, A.B., Kao, C.-F., Hillyer, C., Pikaart, M. and Osley, M.A. (2008) H2B ubiquitylation plays a role in nucleosome dynamics during transcription elongation. *Mol. Cell*, **31**, 57–66.
73. Martens, J.A., Wu, P.Y.J. and Winston, F. (2005) Regulation of an intergenic transcript controls adjacent gene transcription in *Saccharomyces cerevisiae*. *Genes Dev.*, **19**, 2695–2704.
74. Wilusz, J.E., Sunwoo, H. and Spector, D.L. (2009) Long noncoding RNAs: functional surprises from the RNA world. *Genes Dev.*, **23**, 1494–1504.
75. Nourani, A., Robert, F. and Winston, F. (2006) Evidence that Spt2/Sin1, an HMG-like factor, plays roles in transcription elongation, chromatin structure, and genome stability in *Saccharomyces cerevisiae*. *Mol. Cell. Biol.*, **26**, 1496–1509.
76. Venkatesh, S., Li, H., Gogol, M.M., Workman, J.L. and Workman, J.L. (2016) Selective suppression of antisense transcription by Set2-mediated H3K36 methylation. *Nat. Commun.*, **7**, 13610.
77. Korber, P., Barbaric, S., Luckenbach, T., Schmid, A., Schermer, U.J., Blaschke, D. and Hörz, W. (2006) The histone chaperone Asf1 increases the rate of histone eviction at the yeast PHO5 and PHO8 promoters. *J. Biol. Chem.*, **281**, 5539–5545.
78. Williams, S.K., Truong, D. and Tyler, J.K. (2008) Acetylation in the globular core of histone H3 on lysine-56 promotes chromatin disassembly during transcriptional activation. *Proc. Natl. Acad. Sci. U.S.A.*, **105**, 9000–9005.